ESCOLA SUPERIOR NÁUTICA INFANTE D. HENRIQUE

MARITIME ENGINEERING DEPARTMENT

Thesis to obtain the Master of Science Degree in

Maritime Engineering

Towards Sustainable Energy: The Influence of Hydrogen Blending with Natural Gas on Boiler Emissions and Pathways to Decarbonize Industries

António Valadão Dos Santos Sérgio Pessoa

Supervisor: Prof. Sandrina Baptista Pereira

Paço de Arcos

September 2023

Acknowledgements

First and foremost, I would like to thank HyChem and their engineers Mr. Arlindo Carvalho and Mr. Pedro Rodrigues for sharing their expertise in the hydrogen industry, providing key data and access to testing on their equipment.

I would also like to thank Eng. Gonçalo Pereira from Instituto Superior Técnico for the support with the Chemkin software and for sharing his knowledge and experience, and to my supervisor Prof. Sandrina Batista Pereira, for her guidance, trust, availability, and overall support in preparing this thesis.

Finally, for the unconditional support of my family, friends, and girlfriend, Maria Eunice throughout my academic life I can only be grateful.

Resumo

Peritos em alterações climáticas acreditam que a emissão de gases com efeito de estufa provenientes da combustão de combustíveis fósseis é responsável pelas alterações climáticas globais. Para combater o aumento da temperatura média global, estão a ser aplicados regulamentos, mais rigorosos que incidem na eficiência energética, poluição atmosférica e emissões de gases com efeito de estufa, criando desafios a todos os sectores dependentes de combustíveis fósseis, incluído o sector da indústria marítima. Os combustíveis e fontes de energia alternativas são cruciais para atingir a descarbonização do sistema energético mundial e apesar de muitos combustíveis alternativos estarem em fase de desenvolvimento, não se encontram prontos para uma utilização imediata. Uma mistura de hidrogénio e gás natural pode ser um primeiro passo valioso para reduzir as emissões de dióxido de carbono, de óxidos de azoto e de hidrocarbonetos provenientes de instalações industriais. O presente trabalho tem como objetivo analisar os efluentes de uma caldeira alimentada por uma mistura de gás natural e diferentes percentagens de hidrogénio, assim como apresentar uma visão geral de outras alternativas significativas que possam dar novo rumo às indústrias dependentes de combustíveis fósseis.

Palavras-chave: Hidrogénio, Indústria Marítima, Mistura de Combustíveis, Análise de Efluentes, Gases com Efeito de Estufa.

Abstract

Worldwide, climate change experts believe that the emission of greenhouse gases from the combustion of fossil fuels is responsible for global warming. To combat the increase in global temperature, tighter regulations on energy efficiency, air pollution, and emissions of greenhouse gases are being put into force, challenging all carbon dependent sectors, namely the conventional shipping industry. Alternative fuels and energy sources are key to achieve the decarbonization of the global energy system, and although many scenarios of alternative fuels are being considered and developed, they are still not ready for immediate use. A blend of hydrogen and natural gas could be a valuable first step to reduce the emissions of carbon dioxide (CO2), nitrogen oxides (NOx), and hydrocarbons in industrial applications and households. The current project has the goal of analysing the flue gas of a boiler fuelled by a blend of natural gas and different percentages of hydrogen, as well as presenting an overview of other significant alternatives that can reroute the fossil fuel-based industries to a carbon-free course.

Keywords: Hydrogen, Shipping Industry, Fuel Gas Blend, Flue Gas Analysis, Green House Gas Emissions.

Contents

Acknowledgements iii
Resumo iv
Abstract v
Contents vi
List of Figures ix
List of Tables x
Nomenclature xi
Glossary xii
1. Introduction 1
1.1. Topic overview 1
1.2. Objectives 2
1.3. Motivations 2
2. Maritime industry 4
2.1. Propulsion and power generation 4
2.1.1. Marine Diesel Engine Propulsion 4
2.1.2. Diesel-Electric Propulsion 6
2.1.3. Gas turbines 7
2.1.4. Steam engines 8
2.1.5. Boilers 8
2.2. Emission regulations 10
2.2.1. International Maritime Organization 11
2.2.1.1. MARPOL Annex VI 11
2.2.2. United States Government 12
2.2.3. European Union 13
2.3. Alternative Fuels 14
2.3.1. Liquefied Natural Gas 14
2.3.2. Biofuels 15
2.3.3. Renewable Fuels of Non-Biological Origin 15
2.3.4. Methanol 16
2.3.5. Ammonia 16
3. Hydrogen 18
3.1. Properties 18

3.2. Storage 19
3.3. Production 21
3.4. Applications 23
3.4.1. Fuel Cells 24
3.4.2. Combustion in heat engines 27
4. Methodology 31
4.1. Problem Overview 31
4.2. HyChem Boiler 31
4.3. Flue Gas Analysis 32
4.4. Combustion Process Simulation 34
4.4.1. Adiabatic Flame Temperature 35
4.4.2. Flame Speed 36
5. Results 39
5.1. Adiabatic Flame Temperature 39
5.2. Flame Speed 41
5.3. Nitrogen and carbon oxides emissions 42
6. Conclusions and Future Works 45
6.1. Conclusions 45
6.2. Future Works 46
References 47
7. Annexes 52
7.1. Annex A – Technical data Testo 350 52
7.1.1. Technical data Testo 350 analyzer box 52
7.1.2. Technical data CxHy Sensor 53
7.2. Annex B - Adiabatic Flame Temperature Simulations 54
7.2.1. Adiabatic Flame Temperature Simulation Parameters 54
7.2.2. Simulation Nº1 | 100% Natural Gas 55
7.2.3. Simulation Nº2 | 75% Natural Gas – 25% Hydrogen 56
7.2.4. Simulation Nº3 | 50% Natural Gas – 50% Hydrogen 57
7.2.5. Simulation Nº4 | 25% Natural Gas – 75% Hydrogen 58
7.2.6. Simulation Nº5 | 100% Hydrogen 59
7.3. Annex C - Flame Speed Simulations 60
7.3.1. Flame Speed Simulation Parameters 60
7.3.2. Simulation Nº1 | 100% Natural Gas 61

7.3.3. Simulation Nº2 | 50% Natural Gas – 50% Hydrogen 62
7.3.4. Simulation Nº3 | 100% Hydrogen 63

List of Figures

Figure 2.1 – 2-stroke low-speed Wärtsilä RT-flex 82T Diesel engine [16] 5
Figure 2.2 – 4-stroke medium-speed Wärtsilä 50DF engine [16] 5
Figure 2.3 – 4-stroke high-speed Caterpillar C18 Diesel engine [18] 6
Figure 2.4 – Diesel-electric propulsion system installation [19] 7
Figure 2.5 – Aeroderivative gas turbine [20] 7
Figure 2.6 – Water-Tube Boiler [23] 9
Figure 2.7 – Fire-Tube Boiler [24] 10
Figure 2.8 – Reduction in GHG intensity of energy used from 2020 levels [32] 13
Figure 3.1 – Energy density of different fuels [46] 18
Figure 3.2 – Hydrogen's phase diagram [46] 20
Figure 3.3 – Fuel Cell working principle [46] 25
Figure 3.4 – Motor Ferry Hydra [68] 26
Figure 3.5 – Elektra pushboat [69] 27
Figure 3.6 – Crew Transfer Vessel Hydrocat 48 30
Figure 4.1 – Register type Burner [66] 32
Figure 4.2 – Exhaust Funnel 33
Figure 4.3 - Data Collection Set-Up 33
Figure 4.4 - Chemkin | Adiabatic Flame Temperature | Reactor Physical Properties 35
Figure 4.5 – Chemkin | Flame Speed | Reactor Physical Properties 36
Figure 4.6 – Chemkin | Flame Speed | Grid Properties 37
Figure 5.1 – Adiabatic Flame Temperature | Simulations Nº1-5 | Results plotted 40
Figure 5.2 – Adiabatic Flame Temperature 40
Figure 5.3 – Flame Speed | Simulations Nº1,3 and 5 | Results plotted 41
Figure 5.4 – Flame Speed vs Equivalence Ratio 42
Figure 5.5 – Carbon Dioxide Quantities 44
Figure 7.1 - Testo 350 analyzer box technical data [70] 52
Figure 7.2 - CxHy Sensor technical data [70] 53
Figure 7.3 – Annex B | Adiabatic Flame Temperature | Simulation Parameters 54
Figure 7.4 – Annex B | Adiabatic Flame Temperature | Simulation Nº1 | Fuel mixture 55
Figure 7.5 – Annex B | Adiabatic Flame Temperature | Simulation Nº1 | Results plotted 55

Figure 7.6 – Annex B | Adiabatic Flame Temperature | Simulation Nº2 | Fuel mixture 56
Figure 7.7 – Annex B | Adiabatic Flame Temperature | Simulation Nº2 | Results plotted 56
Figure 7.8 – Annex B | Adiabatic Flame Temperature | Simulation Nº3 | Fuel mixture 57
Figure 7.9 – Annex B | Adiabatic Flame Temperature | Simulation Nº3 | Results plotted 57
Figure 7.10 – Annex B | Adiabatic Flame Temperature | Simulation Nº4 | Fuel mixture 58
Figure 7.11 – Annex B | Adiabatic Flame Temperature | Simulation Nº4 | Results plotted 58
Figure 7.12 – Annex B | Adiabatic Flame Temperature | Simulation Nº5 | Fuel mixture 59
Figure 7.13 – Annex B | Adiabatic Flame Temperature | Simulation Nº5 | Results plotted 59
Figure 7.14 – Annex C | Flame Speed | Reactor Physical Properties 60
Figure 7.15 – Annex C | Flame Speed | Grid Properties 60
Figure 7.16 – Annex C | Flame Speed | Simulation Nº1 | Fuel mixture 61
Figure 7.17 – Annex C | Flame Speed | Simulation Nº1 | Results plotted 61
Figure 7.18 – Annex C | Flame Speed | Simulation Nº2 | Fuel mixture 62
Figure 7.19 – Annex C | Flame Speed | Simulation Nº2 | Results plotted 62
Figure 7.20 – Annex C | Flame Speed | Simulation Nº3 | Fuel mixture 63
Figure 7.21 – Annex C | Flame Speed | Simulation Nº3 | Results plotted 63

List of Tables

Table 2.1 – Hydrogen's colour code 21
Table 2.2 – Adiabatic Flame Temperatures [K] by different authors 28
Table 5.1 – Natural Gas composition 34
Table 5.2 – Simulated mixtures compositions 35
Table 6.1 – Natural Gas and Hydrogen Equilibrium Temperature 39
Table 6.2 – Nitrogen Oxides Quantities 43

Nomenclature

α	Hydrocarbons
β	Hydrogen
ρ	Density
$\dot{m}$	Mass Flow Rate
$\dot{V}$	Volumetric Flow Rate
G	Gravimetric Energy Density
P	Power

Glossary

AE	Alkaline Electrolysis
AEM	Anion Exchange Membrane Electrolysis
ATR	Autothermal Reforming
CcH2	Cryo-Compressed Hydrogen
CFD	Computational Fluid Dynamics
CGH2 or CH2	Compressed Gaseous Hydrogen
CODAG	Combined Diesel Engine and Gas Turbine
CODLAG	Combined Diesel-Electric Generator and Gas Turbine
COSAG	Combined Steam and Gas Turbine
CTV	Crew Transfer Vessel
DC	Direct Current
DNV	Det Norske Veritas
ECA	Emission Control Area
ECE	External Combustion Engine
EU	European Union
EEA	European Economic Area
e-LNG	Synthetic Liquified Natural Gas
FC	Fuel Cell
FGR	Flue Gas Recirculation
GHG	Green House Gas
HFO	Heavy Fuel Oil
HT-PEMFC	High Temperature Proton Exchange Membrane Fuel Cell
ICE	Internal Combustion Engine
ILUC	Indirect Land Use Change
IMO	International Maritime Organization
IRA	Inflation Reduction Act
LBG	Liquefied Biogas
LH2	Liquefied Hydrogen
LNG	Liquefied Natural Gas
LPG	Liquefied Petroleum Gas
MARPOL	International Convention for Prevention of Pollution by Ships
MCFC	Molten Carbonate Fuel Cell
MEA	Membrane Electrode Assembly
MEPC	Marine Environment Protection Committee
MSC	Maritime Safety Committee
MF	Motor Ferry
NG	Natural Gas

NH3	Ammonia
NTP	Normal Temperature and Pressure
PEM	Proton Exchange Membrane
PEMFC	Proton Exchange Membrane Fuel Cell
POX	Partial Oxidation
PtL	Power-to-Liquids
RCF	Recycled Carbon Fuels
RE	Renewable Energy
RFNBO	Renewable Fuel of Non-Biological Origin
SH2	Slush Hydrogen
SMR	Steam Reforming
SOE	High-Temperature Solid Oxide Electrolysis
SOFC	Solid Oxide Fuel Cell
ULN	Ultra-Low NOx

1. Introduction

1.1. Topic overview

Global temperature increases are causing disruptions in ecosystems and escalating the unpredictability of atmospheric events. Experts believe that these changes are anthropogenic, being a consequence of the increase in greenhouse gas (GHG) emissions. This is because these gases allow sunlight to pass through the atmosphere but prevent the inherent heat from escaping and consequently contribute to the increase in the global average temperature. The GHGs with the greatest impact on environmental changes are carbon dioxide (CO2), methane (CH4), nitrogen oxides (NOx), and fluorinated gases [1]. Given that climate change is driven primarily by carbon dioxide emissions, it is of the utmost importance to reduce them. To face this issue and in accordance with the prevention of air pollution due to ships, the International Maritime Organisation (IMO) acted in 1997 by adding Annex VI to the International Convention for the Prevention of Pollution by Ships (MARPOL). This annex established rules for the Prevention of Atmospheric Pollution by Ships, and in 2011, it adopted a package of technical measures for new ships and an operational reduction of GHG emissions for all ships [2]. The regulations put in place have received some criticism owing to the frailty of the measure's stringency and the lack of information disclosure [3]. Additionally, it is believed that, by 2050, the percentage of total carbon dioxide annual emissions originated by shipping industry can rise from 2% to 17% due to the increase in maritime transportation demand and the reduction of emissions from other sectors [4] [5]. As a result of increasing media and social pressure and adverse atmospheric events, there have emerged proposals for the introduction of a carbon levy for the shipping industry [6], and consequently, the urge for the decarbonization of the sector has gained vigour. In parallel, the land-based energy sector has been pushed down the decarbonization path due to recent carbon emissions tax price spikes.

Fuels regulation, emission control area (ECA) expansion, and the promotion of energy efficiency are some of the short-term paths already taken by regulatory authorities to start the decarbonization process in the maritime industry. Nonetheless, some companies have gone further and adopted a change from heavy fuel oil (HFO) to liquefied natural gas (LNG) for their new vessel propulsion systems, allowing a reduction of about 20% of CO2, 85% of NOx, 99% of sulphur oxides (SOx), and 99% of fine particle

emissions [7]. However, the lifetime of a merchant vessel is well over 20 years, and about 70% of cargo ships are over 15 years old [8], implying that a large portion of operating merchant vessels were not built to meet the IMO's GHG reduction goals. Since the capital expenditure involved in building a new ship is high, not every company or ship owner has the means to replace their vessels. Still, retrofitting engines and/or installations to consume less carbon-intensive fuel is a viable option. The use of a set percentage of hydrogen with fossil fuels in conventional combustion engines can contribute to the reduction of GHG emissions without reducing the energy efficiency of the engines.

1.2. Objectives

The research objective of this work is to characterise the emissions from hydrogen-natural gas blends and evaluate their environmental impact. It also seeks to determine which types of ships will benefit the most from hydrogen fuel and whether using it on board is feasible.

This being so and given the context of the present work, the following research questions were asked:

- "Can the addition of hydrogen to a natural gas fuelled boiler reduce GHG emissions?"
- "Is hydrogen use onboard ships feasible?"

Before the research, testing, and analysis of the results, it is known that based on the percentage of carbon present in hydrogen, it is expected that carbon-related emissions will be reduced; however, for other emissions such as nitrogen oxides, no hypothesis can be drawn from the beginning. Additionally, regarding the feasibility of using hydrogen onboard ships, no conclusions can be drawn at this point in the project.

1.3. Motivations

Being aware of the relevancy the topic of alternative fuels has within the framework of current technological developments in the maritime sector and knowing there was a possibility to run tests on a boiler, research was conducted to establish a topic yet to be developed.

Existing research on hydrogen-natural gas blends includes integration with existing energy distribution and transportation [9], safety and risk analysis [10], materials and compatibility studies [11], economic feasibility and market adoption [12], life cycle assessment [13], emission reduction and air quality [14], and combustion analysis [15].

While the research studies developed regarding the analysis of combustion and emission reduction of hydrogen-natural gas blends covered both household appliances and internal combustion engines, a research gap was found for the analysis of such blends in boilers.

2. Maritime industry

The maritime industry is a crucial component of global trade and transportation, involving the movement of goods and people across the world's oceans, seas, and waterways. It encompasses a wide range of activities and sectors, each contributing to the efficient and effective functioning of global trade.

These activities can be divided into two groups the shore and the offshore based activities. The first group includes port operations, such as cargo handling, port authorities, logistics and distribution; maritime services, such as classification societies, ship management and maritime law and regulation; shipbuilding and repair which includes ship design and engineering and shipyards; maritime education and training including maritime academies and training centres. These shore-based activities have different power needs; however, their power necessities can be met by the existing power grid. Conversely, the offshore based activities such as merchant shipping, passenger transport, offshore drilling, renewable energy, and commercial fishing, have a limited array of options to fulfil their energy requirements. And why is that? Different activities have different power needs; however, they all need energy for propulsion and power generation for onboard consumption while at sea.

2.1. Propulsion and power generation

Shipping propulsion systems can be diverse, reflecting the needs of the vessels they are installed in, enabling them to navigate and perform various functions efficiently.

2.1.1. Marine Diesel Engine Propulsion

The most commonly used propulsion system onboard includes marine diesel engines, which are a type of internal combustion engine that ignites fuel by injecting it into hot, high-pressure air in a combustion chamber. The diesel engine operates within a fixed sequence of events, which may be achieved either in four or two strokes.

The low-speed two-stroke engine, 70 to 120 rev/min, Figure 2.1, is used for main propulsion units since it can be directly coupled to the propeller and shafting. The largest

transoceanic vessels sailing – container, bulk carriers, RoRos, and tankers – use these engines for main propulsion purposes.

Figure 2.1 – 2-stroke low-speed Wärtsilä RT-flex 82T Diesel engine [16]

The medium-speed four-stroke engine, 250 to 1200 rev/min, Figure 2.2, is used in the large vessels for auxiliaries purposes such as hotel load, pump driver and electrical power generation and for main propulsion with a gearbox on medium to small size vessels such as dredgers, container vessels, .

The more compact high-speed four-stroke engine, above 1250 rev/min, Figure 2.3, is mostly found in smaller vessels for main propulsion coupled to a gearbox.

Figure 2.2 – 4-stroke medium-speed Wärtsilä 50DF engine [16]

A four-stroke diesel engine resembles a gasoline engine as it works on the four-stroke cycle, that is, admission, compression, power, and exhaust. When the piston gets down

on the air admission stroke, the lower pressure in the cylinder allows a charge of air into the cylinder through the inlet valve, which opens just before the top dead centre. Once the piston has passed the bottom dead centre and is beginning to ascend, the inlet valve closes, and the upward movement of the piston compresses the air charge in the cylinder, causing a quick rise in temperature. Before the second stroke is over, the fuel oil is gradually injected into the cylinder by an injector. The burning of the air-fuel charge makes the gases expand, which in turn pushes the piston downward and creates the power stroke. Before the piston reaches the bottom dead centre, the exhaust valve opens, and as the piston goes up again, the burnt gases are forced out through the exhaust valve. Just before the top dead centre, the inlet valve opens, and the cycle begins again [16] [17] [18].

Figure 2.3 – 4-stroke high-speed Caterpillar C18 Diesel engine [18]

When subjected to modifications marine diesel engines can be used as dual-fuel engines, Figure 2.2, which are propulsion systems capable of operating on two different types of fuel, typically diesel and one other fuel such as liquefied natural gas (LNG), hydrogen, methanol, or ammonia. This flexibility allows ships to optimize fuel usage based on availability, cost, and environmental regulations. These types of engines are usually found onboard LNG carriers, cruise ships, ferries, container ships and offshore vessels [16].

2.1.2. Diesel-Electric Propulsion

The diesel electric propulsion combines the benefits of diesel power generation with the precision and control of electric motors. They usually comprise 4-stroke medium

speed diesel engines as power generation units (gensets) for the electric propulsion system, Figure 2.4.

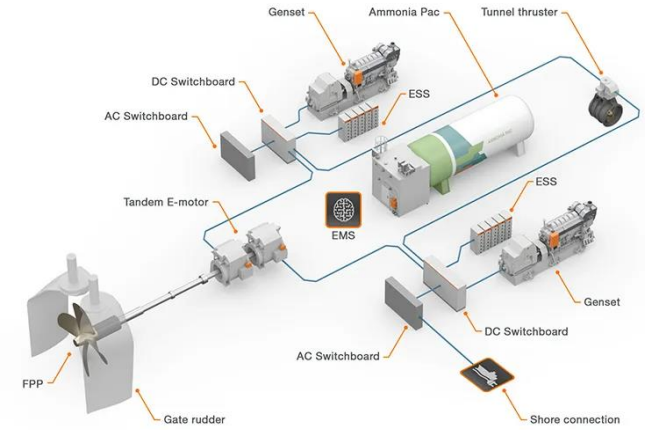

Figure 2.4 – Diesel-electric propulsion system installation [19]

The low noise and vibration, improved reliability, smoother manoeuvring and positioning, easy operation, and fuel savings, mean that this type of propulsion is ideal for tugs, offshore vessels, research and special vessels, and for large cruise ships [19]. Additionally, with new technologies making their way to the market, it will be easier to replace the gensets with new power sources such as a future-fuel operated engine, a battery or a fuel cell.

2.1.3. Gas turbines

Gas turbine propulsion systems provide a powerful and flexible solution for marine purely mechanical propulsion drive configurations or alternatively to generate electricity, which is then used by electric drives to propel the ship. These systems are particularly suited to applications requiring high speed and rapid manoeuvrability such as high-speed

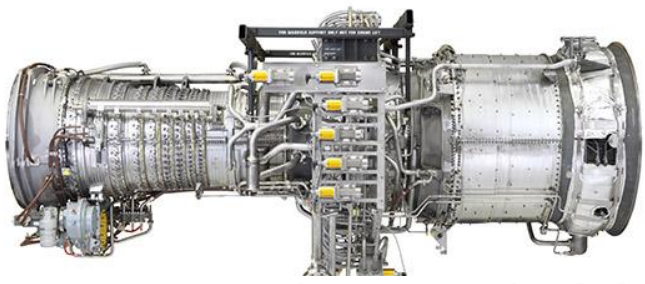

Figure 2.5 – Aeroderivative gas turbine [20]

ferries, luxury yachts and crise ships. While they offer significant advantages in power density and operational response, they come with trade-offs in terms of fuel efficiency and system complexity [20].

To maintain the operational advantages of gas turbines and overcome the poor part load performance, several types of combined power plants are used. They can be combined in a steam and gas turbine arrangement (COSAG), combined diesel engines and gas turbines (CODAG), and combined diesel-electric generators and gas turbines (CODLAG). Their use in combined systems helps mitigate some disadvantages, making them a valuable option for modern maritime applications [21].

2.1.4. Steam engines

Marine steam engines played a crucial role in the development of modern shipping and remain relevant in specific applications such as nuclear-powered ships, large tankers and historical vessels. Their working principle involves generating steam in a boiler, using the steam to produce mechanical energy in a turbine or engine, and then converting this energy into propulsive force.

While largely supplanted by more efficient and flexible propulsion systems, steam engines are still found in certain niche areas, offering unique advantages in power output and operational smoothness.

2.1.5. Boilers

Onboard steam powered vessels boilers play a crucial role as steam producer; however, they can be found practically onboard every ship being used for power generation, auxiliary heating, cargo tank heating, tank cleaning, freshwater generation, auxiliary steam and for domestic purposes.

A boiler is a closed vessel that is used to heat water or other fluids to generate steam or hot water. The steam or hot water produced by a boiler can be used for various applications, including heating, power generation, and industrial processes.

There are several types of boilers, however the most common aboard are the water-tube, the fire-tube, the exhaust gas economizer, and the electric boiler. Onboard ships

with a large power consumption it is usual to see a combination of two or more types of boilers.

In water-tube boilers, Figure 2.6, feedwater flows through tubes that are heated externally by hot gases from the furnace. The heat transfer occurs within the tubes, producing steam. The fast steam generation capacity, high efficiency (for a boiler), ability to handle high pressures and reliability make it one of the most common boilers onboard ships [22].

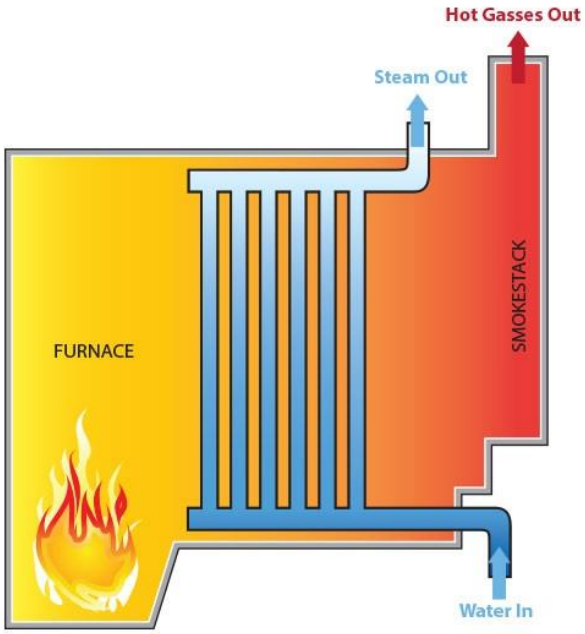

Figure 2.6 – Water-Tube Boiler [23]

Firetube boilers, Figure 2.7, operate by sending combustion gas through a series of straight tubes surrounded by feedwater. Often identified by the number of passes used, this refers to the number of times combustion gas flows the length of the pressure vessel as it transfers heat to the water. Firetube boilers cost typically less up front than water-tube boilers and offer lower operating costs when compared to a similarly sized water-tube boiler, since they are easier to maintain due to better fireside access and their efficient straight tube design [22].

Figure 2.7 – Fire-Tube Boiler [24]

Exhaust gas economizers are water-tube boilers that use the thermal energy of the exhaust gases originated in the combustion process of an engine, boiler, or other industrial process. Exhaust gas economizers are commonly used in marine applications, where they recover heat from the main engine exhaust gases to heat water. By recovering waste heat, they contribute to an increase in the overall efficiency of the system, help reduce emissions by reducing the fuel consumption and consequently saves on fuel costs.

Electrical boilers use electric heating elements to generate heat, they are commonly used to heat smaller amounts of water, mostly for domestic uses, and have high efficiencies.

Except for the electrical type, boilers burn a fuel to convert its chemical energy into thermal energy and while onboard ships they usually burn the same fuel as the auxiliary engines, Low Sulphur Heavy Fuel Oil or Marine Diesel Oil, onshore boilers use or either Naphtha or Natural Gas. Burning fossil fuels means, that boilers are a direct emitter of CO_2, NO_x, SO_x, and particular matter.

2.2. Emission regulations

In the last few decades, the bulk of the maritime industry has been relying on the use of carbon intensive petroleum-based fuels such as marine gas oil, heavy fuel oil, and naphtha; however, in recent years international shipping emissions have been regulated worldwide by the International Maritime Organization (IMO) and more locally by the laws and regulations enforced by local governments, such as the United States government and the European Union.

2.2.1. International Maritime Organization

The IMO is a specialized agency of the United Nations responsible for regulating shipping on a global scale having 175 member states and 50 conventions and protocols. The IMO's primary goal is to ensure the safety and security of shipping, and the prevention of marine and atmospheric pollution by ships [25].

The IMO's regulatory framework includes various conventions, the most notable being the International Convention for the Safety of Life at Sea (SOLAS) and the International Convention for the Prevention of Pollution from Ships (MARPOL). These conventions, along with others, form the basis for the global regulatory framework governing maritime safety, security, and environmental protection [26].

MARPOL stands for the International Maritime Organization's International Convention for the Prevention of Pollution from Ships, 1973, as modified by the Protocol of 1978 here relating to (MARPOL 73/78). It is one of the most important international agreements regulating the prevention of pollution from ships and aims to minimise pollution of the seas, including pollution by oil, chemicals, harmful substances in packaged form, sewage, garbage, and air pollution from ships [27].

2.2.1.1. MARPOL Annex VI

The convention consists of six annexes, each addressing a specific type of pollution, including the prevention of pollution by oil; by noxious liquid substances; by harmful substances carried by sea in packaged form; by sewage and garbage from ships; and the prevention of air pollution from ships.

Annex VI, focuses on reducing air pollution from ships by setting limits on sulphur and nitrogen oxide emissions, as well as other air pollutants. The annex also includes regulations on energy efficiency and the use of alternative fuels [28].

MARPOL Annex VI sets limits on the sulphur content of fuels used by ships. The most recent amendments, known as IMO 2020, significantly lowered the global sulphur cap from 3.5% to 0.5% m/m (mass by mass) for fuel oil used on board ships, with certain designated emission control areas (ECAs) having even stricter limits (0.1% m/m). Emission Control Areas, as defined in Annex VI, are specific geographical areas where more stringent emission standards apply to address air quality concerns. ECAs include the Baltic Sea, North Sea, North American ECA, and the U.S. Caribbean Sea [28].

The Nitrogen Oxide (NOx) Emission Limits regulation includes Tier I, Tier II, and Tier III standards that define maximum NOx emission levels based on the engine's construction date and its location (ECAs). Tier III standards, which are the strictest, apply to newly built ships in ECAs, significantly limiting NOx emissions compared to previous tiers. The limits are given in grams per kilowatt-hour (g/kWh) [28].

Annex VI also addresses the emission of particulate matter, setting limits on the mass concentration of particulate matter in the exhaust gas of ship engines [28]. Particulate matter emissions refer to tiny, solid particles and liquid droplets that are suspended in the air. These particles vary in size, composition, and origin, and they can have significant effects on air quality and human health [29].

Amendments introduced by MEPC 76 in 2021 include regulations related to the Energy Efficiency Existing Ship Index (EEXI) and the Carbon Intensity Indicator (CII). These measures aim to improve the energy efficiency of existing ships and set carbon intensity targets for ships, respectively [28].

The Ship Energy Efficiency Management Plan (SEEMP) is a mandatory plan that outlines measures to improve the energy efficiency of a ship's operation. It includes guidelines for monitoring and improving energy efficiency [28].

A mandatory data collection system for fuel consumption is in place to collect and report data on ship’s fuel consumption, which is used to establish benchmarks and assess the energy efficiency of international shipping [28].

These measures collectively aim to reduce the environmental impact of shipping operations, improve air quality, and contribute to global efforts to combat climate change.

2.2.2. United States Government

The United States Government signed in a reconciliation package, the Inflation Reduction Act (IRA), allocating nearly $369 billion for action related to climate change. The IRA will provide benefits that significantly reduce alternative fuel production costs, since it encompasses a tax credit scheme for producers of renewable fuels and funding for infrastructure development for fuel producers whom provide higher blends of such fuels [30] [31].

2.2.3. European Union

The European Union (EU) has incentivised the use of renewable and low-carbon fuels on vessels to reduce greenhouse gas emissions through the adoption of the FuelEU Maritime Regulation. This regulation will provide legal certainty for ship operators and fuel producers and increase the demand for, and consistent use of, renewable and low-carbon fuels, reducing the greenhouse gas emissions from the shipping sector [32].

FuelEU Maritime Regulation sets requirements for a gradual reduction of annual average GHG intensity of energy used by ships trading in the EU or European Economic Area (EEA), Figure 2.8 – Reduction in GHG intensity of energy used from 2020 levels Figure 2.8, measured as GHG emissions per energy unit (gCO2e/MJ). This will start at a 2% reduction in 2025, increasing to 6% in 2030, and accelerating from 2035 to reach an 80% reduction by 2050 [33].

GHG emissions are calculated in a well-to-wake perspective, including emissions related to extraction, cultivation, production and transportation of the fuel, in addition to emissions from energy used on board the ship.

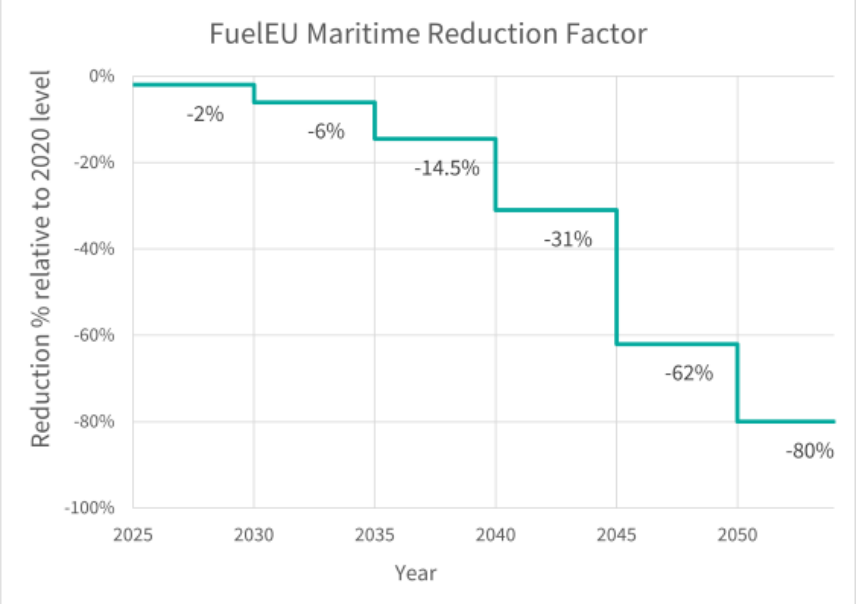

Figure 2.8 – Reduction in GHG intensity of energy used from 2020 levels [32]

The GHG intensity requirement applies to 100% of energy used on voyages and port calls within the EU or EEA, and 50% of energy used on voyages into or out of the EU or EEA.

In addition, to incentivise zero-emission port stays, passenger and container ships will be required to connect to onshore power supplies at major EU ports from 2030 and all EU ports with onshore power supplies from 2035. This will not be the case for very short stays, less than 2 hours or if the ship uses zero-emission technology whilst at berth. Any port infringements will also be subject to financial penalties. The revenues generated from the regulation's implementation FuelEU penalties, will be used for projects in support of the maritime sector's decarbonisation with an enhanced transparency mechanism [34].

While the Annex VI from MARPOL will penalize inefficient and high GHG emitting vessels, the IRA subsidies will incentivise the production and consumption of alternative fuels, and the FuelEU will progressively raise the cost of conventional fossil fuels, increasing the demand of low GHG intensity fuels, such as biofuels, bio gas, renewable fuel of non-biological origin (RFNBO), and recycled carbon fuels (RCF) [35].

2.3. Alternative Fuels

As key regulations, such as Annex VI's Tier III NOx emissions standards, the Inflation Reduction Act, and FuelEU start to make an impact it is certain that alternative fuels will make their way into the markets, such as liquefied natural gas, biofuels, renewable fuels of non-biological origin (RFNBO), methanol, ammonia, and hydrogen – which will be discussed in chapter 3.

2.3.1. Liquefied Natural Gas

Liquefied natural gas (LNG) is a cleaner-burning fossil fuel that allows a reduction of about 20% of CO2, 85% of NOx, 99% of sulphur oxides (SOx), and 99% of fine particle emissions [7], when compared with conventional carbon-based fuels. It is commonly used as a fuel in vessels with dual-fuel power generating systems, whether diesel-electric or combined gas turbine systems.

As a ship fuel, LNG is interchangeable with renewable LBG (liquefied biogas, also called bio-LNG), which produces up to 90% less carbon dioxide emissions than conventional fuel. In the future, there will be renewable synthetic LNG (e-LNG) available which is chemically identical to LNG and LBG. The potential

of renewable LBG and e-LNG is significant. There is excellent availability of liquefied gas and a well-developed infrastructure for distributing the fuel. Since both LNG and LBG consist of methane, companies can switch to, switch between, or blend the fuels [36].

2.3.2. Biofuels

Unlike other renewable energy sources, biomass can be converted directly into liquid fuels, called "biofuels," to help meet transportation fuel needs. The two most common types of biofuels in use today are ethanol and biodiesel, both of which represent the first generation of biofuel technology. Onboard ships biodiesel is the chosen biofuel to replace or be blended with diesel oil.

Biodiesel is a liquid fuel produced from renewable sources, such as new and used vegetable oils and animal fats and is a cleaner-burning replacement for petroleum-based diesel fuel. Biodiesel is nontoxic and biodegradable and is produced by combining alcohol with vegetable oil, animal fat, or recycled cooking grease [37].

While biofuels are important in helping greenhouse gas reduction targets, biofuel production typically takes place on cropland that was previously used for agriculture, to grow food or feed. Since this agricultural production is still necessary, biofuel production may lead to the extension of agricultural land into non-crop land, possibly including areas with high carbon stock, such as forests, wetlands and peatlands. This process is known as indirect land use change (ILUC). As it may cause the release of CO2 stored in trees and soil, ILUC poses a risk to the greenhouse gas savings that result from increased production of biofuels [38].

2.3.3. Renewable Fuels of Non-Biological Origin

The term Renewable Fuels of Non-Biological Origin is an umbrella term for all gaseous and liquid renewable fuels that do not rely on biomass. The main technology to produce these RFNBOs is the use of electrolysis powered by renewable electricity to produce hydrogen. This hydrogen can be combined with nitrogen to produce ammonia or with carbon to produce various synthetic hydrocarbons, such as e-methanol, e-kerosene, e-diesel and e-gasoline, also known as Power-to-Liquids (PtL) [39].

The main advantage of RFNBOs is that scaling them up will use far less land and water compared to biofuels. Nevertheless, charging electric batteries with (renewable) electricity directly will be far more efficient than converting the electricity in hydrogen and e-fuels. However, deep sea shipping demands large amounts of power that batteries cannot provide and that's where the higher energy density of RFNBO will play its part [40].

2.3.4. Methanol

Methanol is a safe, proven, cost-competitive marine fuel for the commercial shipping industry that can meet or exceed current and planned emissions regulations. One of the unique and important qualities of methanol compared to other alternative fuels is it is a liquid fuel under ambient conditions. This makes methanol easy to transport, store, and bunker using standard safety procedures that are like the well-established procedures for diesel. Therefore, the cost of converting diesel engines to methanol dual-fuel vessels and land-based infrastructure to store and supply methanol is significantly lower than other alternative fuels that require pressurization or cryogenics. Methanol also has a higher volumetric energy content than alternative fuels like ammonia or hydrogen, making it a better choice for a wide range of vessel types and longer voyages, as it requires less frequent bunkering. In the short term, conventional methanol reduces greenhouse gas emissions from combustion, while in the longer term, green methanol (production powered by renewable energy) can enable the industry to meet the International Maritime Organization's decarbonization goals, since Methanol can reduce SOx and PM emissions by more than 95%, and NOx by up to 80% compared to conventional marine fuels [41].

As green methanol is chemically identical as conventional methanol, there are no compatibility issues or further engine investment required by shipping companies, allowing a seamless, gradual transition to lower CO2 emissions.

2.3.5. Ammonia

Ammonia (NH_3) is a compound composed of nitrogen and hydrogen. It is a colourless gas with a pungent odour, widely used in various industrial applications, including as a fertilizer, refrigerant, and in the production of chemicals. Recently, ammonia has gained

attention as a potential alternative fuel due to its energy density and capability to be produced and used with minimal carbon emissions.

Almost all ammonia in use today is made from hydrocarbons, and as such confers almost no carbon abatement advantage, while simply adding costs. By contrast, green ammonia – produced by electrolysis powered by renewables or nuclear – is an excellent source of zero-emission fuel, provided that associated NOx emissions are managed appropriately.

Onboard ships, ammonia can be used as a fuel in specially modified combustion engines, in gas turbines and in fuel cells for electricity generation. However, ammonia is toxic, so the safety of the whole vessel must be considered, including the ventilation systems, additionally, when using ammonia, ships will need larger fuel storage capacity compared to diesel or LNG because ammonia has a lower volumetric energy density than both of these fuels.

Ammonia holds significant potential as part of a diversified approach to reducing greenhouse gas emissions and achieving sustainable energy goals. Ongoing research and development aim to address its challenges and improve the efficiency and safety of ammonia-based energy systems. As renewable energy sources become more prevalent, green ammonia could play a crucial role in decarbonizing various sectors, particularly maritime transport [42].

3. Hydrogen

3.1. Properties

Hydrogen is the simplest and most abundant element in the universe, and due to its high reactivity, it is not possible to find a pure molecule of it naturally on the Earth's surface. Nevertheless, H_2 is pointed out as one of a few promising options to fuel the decarbonization process since it is carbon-free and has a high specific energy content. It is then important to analyse the characteristics that make it so attractive and the methods for its production, storage, and usage.

The gravimetric energy density of an energy source determines its energy content by mass unit. Hydrogen has a gravimetric energy density of about 120 MJ/kg (megajoule per kilogram) while other fuels, such as methane and fuel oil, exhibit much lower values of around 50 MJ/kg and 40 MJ/kg, respectively [43].

However, the volumetric energy content of hydrogen is an obstacle to its usage due to its low density. Figure 3.1 shows the volumetric and gravimetric energy density of different fuels. At normal temperature and pressure conditions (NTP), 20°C, and 1 atmosphere, the density of hydrogen is 0.083 kg/m^3 (kilogram per cubic metre) [44], while methane has a density of around 0.657kg/m^3, and fuel oils have a density range with values varying from 750 kg/m^3 to 1010 kg/m^3 in the case of low-quality heavy fuel oils [45].

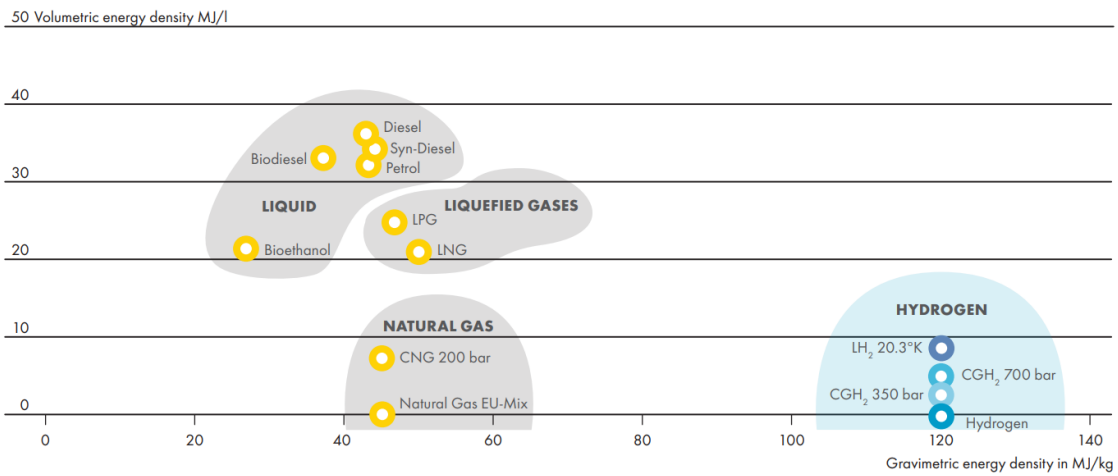

Figure 3.1 – Energy density of different fuels [46]

Hydrogen's low density makes it an energy-poor element by volume, having a volumetric energy density of just 0.01 MJ/l (megajoule per litre), meaning that in NTP conditions to store the same amount of energy, it is required a much bigger space for hydrogen than for other fuels.

3.2. Storage

In the past few years, progress has been made in the research and development of material-based hydrogen storage technologies; however, the most commonly used and matured hydrogen storage methods are still the physical storage methods, which include compression, cooling, or a mixture of both.

Material-based methods rely on chemical absorption and physical adsorption to store hydrogen as liquid- or solid-state compounds. Even though these methods do not have any commercial relevance, their ideal characteristics for storage purposes, safety, and ease of operation make them the most feasible solution for the future [47]. They include, among others, metal hydrides, nanomaterials, liquid organic hydrogen carriers, ammonia, and zeolites [48].

Regarding compressing methods, compressed gaseous hydrogen (CGH_2 or CH_2) can be handled at different gas pressures, ranging from low-pressure storage at 50 bar to high-pressure storage at up to 1000 bar. High-pressure storage requires special steel or composite pressure vessels. In the mobility sector, the storage pressures are between 350 bar and 700 bar and allow for a specific energy density increase from 0.01 MJ/l to 2.9 MJ/l and 4.8 MJ/l, respectively. The compressed hydrogen methods have some operational constraints due to the safety issues brought by the high operating pressures.

Liquefaction increases hydrogen's density by a factor of around 800; however, hydrogen has a very low boiling point, -252.76 °C or 20.3 K; below this temperature, it is liquid under normal pressure of 101.3kPa; above this point, it is gaseous [49]. Figure 3.2 shows the hydrogen's phase diagram. It can be verified that the vapour-pressure curve of hydrogen is very steep and short; in this sense, liquefaction takes place primarily by cooling and less so by compression, and it involves a complex technical refrigeration plant and extra economic cost. Liquefied hydrogen (LH_2) has a volumetric energy density of 8.5 MJ/l, which is quite inferior to the ones of the liquefied gases LNG and LPG, which are 21.0 MJ/l and 25.3 MJ/l, respectively. Even though tanks for LH_2 are mostly used in

the space travel industry, it is believed that LH_2 will be the frontrunner for coastal and sea shipping applications due to the high energy requirements [43].

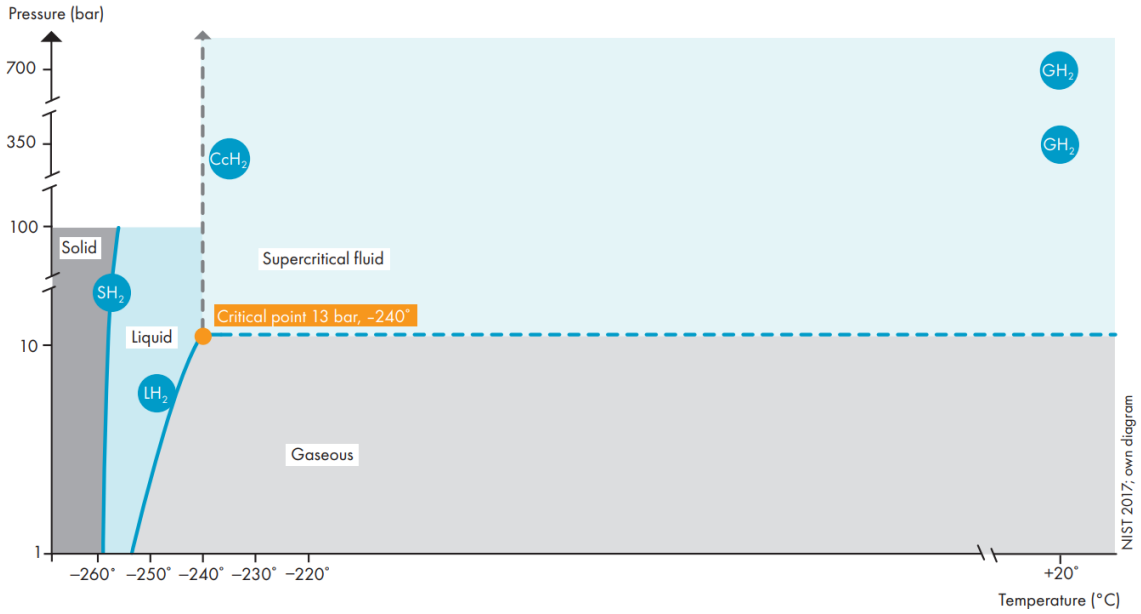

Figure 3.2 – Hydrogen's phase diagram [46]

Besides cooling and compressing methods for hydrogen storage purposes, there is also a combination of both methods. The cryo-compressed hydrogen (CcH_2) is cooled to temperatures close to the critical temperature (approx. 40 K) and is then compressed to approximately 300 bar. According to Gay-Lussac's law, an ideal gas held at constant pressure when cooled will experience a proportional reduction in volume; that is the reason why hydrogen is cooled first [50]. Cryo-compressed hydrogen has a higher energy density when compared with liquefied hydrogen; however, the compression requires an additional energy input. The very low temperatures increase the cost of the cryo-compressing storage method.

Even though it still has no practical usage, slush hydrogen (SH_2) has been tested in launch vehicle propellant; it is roughly composed of solid and liquid hydrogen in equal proportions, and it allows for bigger storage densities when compared with liquefied hydrogen [51].

Although storage methods currently display constraints regarding cost, environmental friendliness, leakage tightness, and density, it is expected that the maturity

of existing techniques and the research and development of new ones will eradicate those drawbacks.

3.3. Production

Hydrogen's zero-carbon emissions at end-user make it particularly appealing for the decarbonization process. To be considered clean energy, the energy source and conversion process must have low GHG emissions. A colour code was developed to facilitate the environmental assessment of hydrogen's source or type. Table 3.1 summarises the hydrogen colour table. It is important to note that there is no international convention on the colour codes, and the definitions may change between countries [52]. Primary energy sources to produce hydrogen include nuclear energy, natural gas, brown coal (lignite), black coal, and renewable energies (RE) such as solar, biomass, algae from sunlight, wind, hydro, geothermal, and tidal.

Currently, there is a surge in investment in large-scale green hydrogen production plants [53], [54] and [55]. Regardless, to this date, roughly 95% of global production is based on fossil fuel sources, and the remaining 5% is related to the production by electrolysis of water with electricity from various sources [56]. It is nonetheless expected that hydrogen production from electrolysis will rise significantly due to the increase in surplus electricity produced by renewable sources. Hydrogen production from fossil fuels is mostly done in large and medium-scale plants, especially refineries, while production from RE is currently mostly done in small, distributed units located at or close to the end user, such as refuelling stations or stationary power sites.

Table 3.1 – Hydrogen's colour code

Colour Code	Primary Energy	Conversion process	GHG footprint
Green	Wind/Solar/Hydro/Geothermal/Tidal	Electrolysis	Minimal
Pink	Nuclear		
Yellow	Mixed-source grid energy		Medium
Blue	Natural Gas/Coal	Natural gas reforming + CCUS Gasification + CCUS	Low
Turquoise	Natural Gas	Pyrolysis	Low
Grey		Natural gas reforming	Medium High
Brown	Brown Coal (lignite)	Gasification	High
Black	Black Coal		

Current hydrogen production methods are based on thermochemical conversion, biochemical conversion, and water electrolysis. Thermochemical methods are the most mature technology and consist of the reforming of fossil hydrocarbons, alcohols, and an oxidant into hydrogen through chemical processes at high temperatures (thermochemical) and with the cooperation of a catalyst. The three main thermochemical processes – steam reforming (SMR), partial oxidation (POX), and autothermal reforming (ATR) – differ in the oxidant used. Thermochemical methods can also be based on the gasification or pyrolysis of solid or liquid biomass, even though they have very low market relevancy; these methods are like the ones already executed in oil refineries and are still more costly when compared to fossil fuels; since, they are heavily dependent on the availability of biomass in the form of wood and stalks, they only make sense if used in areas where biomass is available and does not contribute directly to deforestation [57].

The most commonly used thermochemical method, SMR, uses water vapour and natural gas or other light hydrocarbons and requires additional heat to complete the reaction, emitting, as a consequence, large amounts of CO_2 [58]. Oxygen and heavy hydrocarbons are used for POX, which occurs at high temperatures and high pressure; additionally, it emits carbon monoxide and carbon dioxide; and furthermore, it offers a lower global process efficiency [59]. The last reforming method, ATR, consists of a combination of steam reforming and partial oxidation. The advantage of not being dependent on an external heat supply is offset by the increased investment and operating costs of the air separation unit and the more complex flue gas purification process [58].

$$H_2O \rightarrow H_2 + {}^{1}/_{2}\, O_2 \qquad (1)$$

Water electrolysis is a two-century-old method of producing hydrogen; despite that, only recently has it regained interest the growing necessity of cutting carbon emissions and due to the increase in renewable energy availability. It consists of the dissociation of water (H_2O) into hydrogen (H_2) and oxygen gas (O_2), Equation (1), caused by a direct current (DC) applied by two electrodes submerged in water. The product gases are separated by a membrane, and due to the poor conductivity of water, an electrolyte or

ionic conductor is added. Electrolysers are individual electrolytic cells; if the need to increase production arises, the cells need to be stacked, forming electrolyser stacks [60].

There are different electrolyte systems developed for water electrolysis, and although they differ in electrolyte materials and operating temperatures, the operating principles are the same. These systems include the low-temperature alkaline electrolysis (AE), proton exchange membrane electrolysis (PEM), anion exchange membrane electrolysis (AEM), and high-temperature solid oxide electrolysis (SOE). Currently, the efficiency of water electrolysers is around 60% to 80%, and only low-temperature solutions are available on the market, with AE responsible for the biggest market share. It is seen as though they are cheap, relatively stable, and produce hydrogen with high purity; however, these electrolysers generate an alkaline fog that contaminates the gas produced; additionally, they cannot start up quickly and have a slow response time, making them a bad solution for an electrolyser to be fed by unreliable renewable energy sources [61]. Although PEMs are more environmentally friendly, have a fast response time, have a compact design, and are commercially available, they are only used in medium and small applications with less than 300 kW of power. Moreover, these electrolysers have a shorter lifespan and consequently a higher global cost. AEM electrolysers have just arrived on the market and are only available for limited applications, while the high-temperature SOE is still in the experimental stage in laboratories [62].

Today, water electrolysis still lacks economic competitiveness when compared with the matured hydrogen production options on the market and this is due to its dependency on electricity prices. However, it is expected that with the development of efficiency, operating life, electrolyser size, adaptability to volatile power supplies, and power density, water electrolysis will become more economically attractive. The increase in carbon taxes will increase the cost of the more mature market options and enhance the attractiveness of water electrolysis.

3.4. Applications

The growing need to shift from fossil fuels has increased the number of applications of hydrogen; however, to the present date, it has mainly been used for material and energy applications.

The most important industrial areas of material applications of hydrogen involve special processes that include further processing or refining of other substances with the aid of hydrogen combined with pressure, temperature, and catalysts. These include the synthesis of ammonia, the hydrotreating and hydrocracking of oil products in refineries, the synthesis of methanol, and other chemical and industrial applications that include the production, of base materials for paints and synthetic fibres, metalworking, flat glass production and in the electronics industry as a protective and carrier gas.

As for power generation, hydrogen can cover a range of applications, such as industrial and domestic stationary power generation and mobility, powering either internal combustion engines (ICEs), external combustion engines (ECEs), or fuel cells (FCs). FCs are the main use of hydrogen as a fuel, and even though it is used in ICEs, mostly in dual fuel systems, it is not common [63].

Regarding maritime applications, the use of hydrogen-based fuels in shipping is very limited since ships have large power needs and high fuel requirements. However, hydrogen is used mostly in short-sea and short-distance shipping that operates inside Emission Control Areas, as well as auxiliary engines and/or hotel loads [43]. This is primarily due to the low availability of hydrogen fuel, local regulations and requirements, and funding. The change to hydrogen as a fuel relies on the existence of bunkering infrastructure in the ports, as well as on-board fuel storage and equipment ready to consume it.

3.4.1. Fuel Cells

Fuel cells are the most attractive form of hydrogen consumption owing to their high energy efficiencies and modular capabilities; however, the maritime industry poses specific challenges that make their adoption difficult, namely a difficult working environment and restrictions with onboard energy storage. Nonetheless, fuel cells may be used on merchant ships for low-power demand primary propulsion, auxiliary power for hybrid propulsion, energy generation, and emergency power supply.

Though an individual fuel cell only produces a small electric potential, a connection of cells in series, i.e., fuel cell stacks, can be used to achieve the necessary power demands. The process that occurs in a fuel cell is the reverse of electrolysis, Figure

3.3, i.e., the production of direct current and the formation of water through the reunion of oxygen and hydrogen.

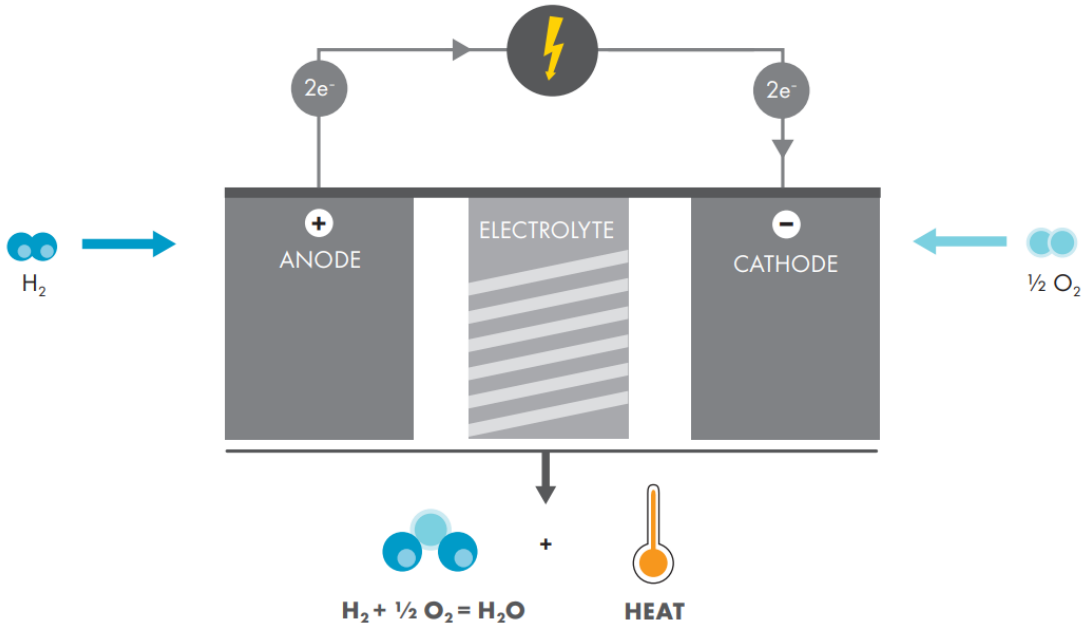

Figure 3.3 – Fuel Cell working principle [46]

Different fuel cells can operate at three distinct ranges of temperatures and with different membrane electrode assembly (MEA) or electrolytes, since the latter define their performance. A lower-operating-temperature fuel cell requires a higher-purity hydrogen supply. The efficiency of the FC increases if the cathode is supplied with pure oxygen instead of air, and the overall efficiency also rises if a recovery heat system is utilised.

Due to the high operating temperatures, HT-PEMFC, MCFC, and SOFC have higher efficiencies since they can include heat recovery systems; additionally, they can run a broader range of fuels, including hydrogen with inferior purity. Even though they have advantages, the high working temperatures mean that start-up times are longer and that the materials used need to be capable of withstanding higher temperatures and to be corrosion-resistant [64] [65].

The PEMFC is of high-power density, small volume, quick start-up, and allows for flexible and safe operation; nevertheless, it requires pure hydrogen to prevent carbon monoxide and sulphur poisoning, and a complex water management process is required, meaning it requires a substantial initial investment [66].

The proton exchange membrane (PEMFC/HT-PEMFC), molten carbonate (MCFC), and solid oxide fuel cells (SOFC) are the most promising choices for maritime applications in terms of energy efficiency, power capacity, and sensitivity to fuel and oxidant impurities. The technical progress of fuel cells has taken large steps recently, allowing them to achieve higher overall efficiencies. Since the beginning of the century, there have been several projects of marine fuel cell systems powered by hydrogen with capacities ranging from 10 kW to 120 kW, being only able to power vessels such as small river push boats, small ferries, and small pleasure crafts [62]. However, recently, projects with hydrogen marine fuel cell stacks have offered capacities reaching MW [67].

In Norway, early this year, the Det Norske Veritas (DNV) classed motor ferry (MF) Hydra, Figure 3.4, started sailing using two 200kW PEM FC running on liquid hydrogen, stored in an 80 cubic metre tank. The liquid hydrogen is produced in Germany by Linde's 24 MW electrolyser using PEM technology to produce green hydrogen and supplied by truck. While running on green hydrogen, the ferry will reduce its CO_2 emissions by up to 95% when compared to running on diesel [68].

Figure 3.4 – Motor Ferry Hydra [68]

In 2021, the pushboat Elektra, Figure 3.5 started sailing in Germany, using 3x100kW HT-PEMFC running on 750 kg of green GH_2 stored at 500 bar. The waste heat

from the fuel cells is used for heating the accommodations and batteries during the winter [69].

Figure 3.5 – Elektra pushboat [69]

Outside of the marine sector, FCs are one of the leading conversion technologies for hydrogen consumption for energy purposes.

3.4.2. Combustion in heat engines

For more than two centuries, the use of hydrogen as a fuel in heat engines has been studied and tested. In 1806, the first internal combustion engine built by Swiss engineer Francois Isaac de Rivaz, was powered not by gasoline but by a mix of hydrogen and oxygen [70]. Even though early efforts were sporadic and mostly limited to the laboratory, there is currently a renewed interest due to its ability to give long-term answers to the energy-environment challenges. Having familiar technology, already-existent manufacturing processes, being reliable, delivering environmental benefits, and not requiring hydrogen with high purity makes the transition into hydrogen engines operationally and economically viable.

The combustion characteristics of hydrogen induce some constraints on its use in internal and external combustion engines since they differ from the properties of the carbon-based fuels commonly used. Hydrogen’s high adiabatic temperature, wide range

of flammability, low ignition energy, small quenching distance, high autoignition temperature, high flame speed at stoichiometric ratios, high diffusivity, and very low density mean that combustion engines need to have some modifications to their fuel delivery system, ignition system, and crankcase ventilation (in the ICEs case) to burn pure hydrogen.

Due to H_2's wide range of flammability, hydrogen engines may operate in a variety of equivalency ratios, from ultra-lean to stoichiometric settings. However, when operating within a specific range of lean operation, the engine provides maximum thermal efficiency, little NOx emissions, and no backfire concerns. Additionally, if the fuel is made up of gas and has a low concentration of hydrogen, in the range of 5% to 20% by volume, the heat engine does not require any change in its components [71].

The adiabatic flame temperature of a mixture is the temperature it will reach when burning under ideal conditions. The adiabatic flame temperature is a function of the different input gases, their masses, and their temperature, as well as the specific heat capacity of each gas, additionally the measuring technics used have some influence on the results; hence, different authors attribute different adiabatic flame temperatures to similar mixtures, as can be seen in Table 3.2 [72].

Table 3.2 – Adiabatic Flame Temperatures [K] by different authors

	Authors			
	[48]	[49]	[50]	[51]
Fuel				
Hydrogen	2527	2483	2400	2318
Natural Gas	2233	-	-	-
Methane	2236	2236	2328	2248
Propane	2253	2250	-	2253

When a mixture of hydrogen and air is burned in a compression engine, the autoignition temperature is a crucial factor in determining the compression ratio of the engine. Since hydrogen has a high autoignition temperature, it is difficult to ignite it in compression engines. However, its low ignition energy allows it to promptly ignite in lean mixtures, making it a far more suitable fuel for Otto cycle engines. The low ignition energy also means that hot spots on the cylinder can serve as sources of ignition and create

problems of premature ignition and flashback [77]. Flashback occurs when the gas velocity exiting the burner nozzle or injector valve is slower than the flame speed of the fuel and can lead to the impairment of injection components [78]. Lean hydrogen mixtures are one way to prevent the occurrence of flashbacks when burning pure hydrogen.

While hydrogen's high diffusivity facilitates the formation of a uniform mixture of fuel and air, it also means that, in the event of a leak, it disperses rapidly. When the high diffusivity is paired with a small quenching distance, i.e., the distance the flame travels from the cylinder wall, the susceptibility of combustion in the crankcase increases. To prevent such phenomena crankcase ventilation is often required.

The laminar flame speed is the relative speed between an unburned gas mixture and the flame front. It depends on the fuel type, air-fuel ratio, temperature, and pressure. Since the combustion system is fixed to the flame, all velocity solutions are relative velocities with respect to the flame front in boilers. At high percentages of hydrogen in premix-type burners, the susceptibility to flashback occurrence rises due to the increased flame speed [78].

When compared to FCs, HICEs achieve low efficiencies [79]. Additionally, they are a source of NOx and close to zero CO_2 emissions. There are nevertheless some advantages to their use, especially when applied to the automotive and maritime transport sectors. The manufacturing processes, facilities, and know-how already exist and do not require a major investment to alter production [80]. Even though there are hydrogen-powered ICEs in maritime applications there are no applications, for hydrogen-powered external combustion engines.

Early in 2022, the crew transfer vessel (CTV) Hydrocat 48, Figure 3.6, was the first of its kind to be powered by two MAN's dual-fuel V12 marine engines rated at 750 kW each, allowing for a reduction of CO_2 emissions of up to 80% whilst maintaining the same power output and autonomy. The CTV Hydrocat 48 is bunkered daily with 200 kg of green GH2 stored at 350 bar in three separate tanks. The green hydrogen is produced with excess wind power. The V12 marine diesel engines were retrofitted for dual-fuel operation; having suffered minimal changes and being compliant with IMO Tier III emissions standards, which limit NO_x emission ranges. They provide the lowest cost and highest reliability for the highest CO_2 reduction [81].

The supplier of the CTV Hydrocat 48 propulsion system and major player in the maritime propulsion sector, MAN, has compared ICE technologies with gas turbines, proton exchange membrane (PEM) and solid oxide (SOFC) fuel cells across a variety of parameters and believes hydrogen ICEs offer a more appealing option than fuel cells due to cost, power density, fuel flexibility, and reliability advantages. Moreover, the lifetime of an ICE, with regular maintenance, far outlasts that of a fuel cell stack [43].

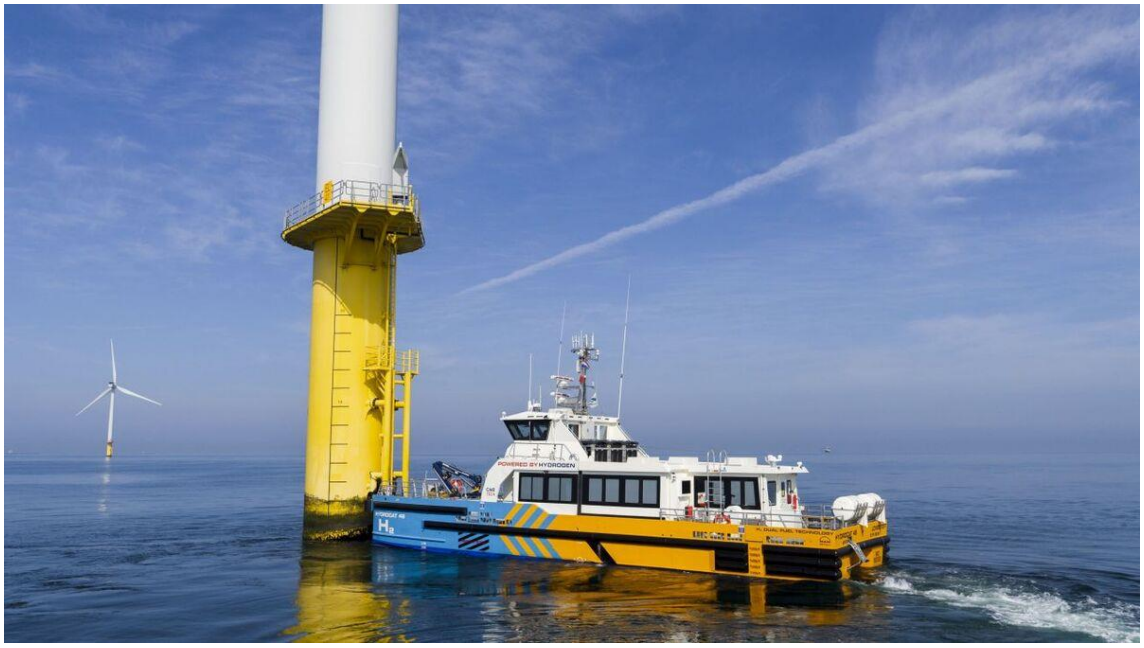

Figure 3.6 – Crew Transfer Vessel Hydrocat 48

Furthermore, the president of the world's biggest automaker, Toyota Motor Corp., Aiko Toyoda, defends hydrogen internal combustion engines, believing different emissions-reducing vehicle technologies are needed for different regions of the world [82].

4. Methodology

4.1. Problem Overview

The increase in fuel cost instability and carbon tax pushes industrial users to consider alternative fuel sources; in some cases, instead of flaring or releasing the left-over hydrogen from different reforming and refining processes, it is blended and burned with the fuel gas.

The present project aims to compare the combustion emissions of a boiler when burning natural gas, hydrogen, or a blend of both.

To achieve such a goal, a collaboration agreement was reached with a company specialised in the hydrogen chemistry industry, HyChem S.A. Being an active element in the transition to a carbon-neutral industry, HyChem allowed the execution of emission tests on a steam generator consuming natural gas, hydrogen, and a mix of both fuels.

The hydrogen used by HyChem, together with sodium chlorate, are co-products in the process of brine electrolysis. Since the H_2 has a high degree of purity, it is not subjected to any final purification stage before being consumed. The hydrogen is not subjected to any of the storage processes described previously; it is supplied to the boiler at approximately 0.15 bar and at ambient temperature.

4.2. HyChem Boiler

The water tube steam generator is composed of a boiler, a steam superheater, an economizer, and a deaerator. The boiler, with a maximum working pressure of 12 bar and a maximum steam production of 3000 kg/h, was built in 2013, originally designed to burn natural gas. The burner was later retrofitted to be compatible with hydrogen's combustion characteristics and ensure safe and optimal operation. Since hydrogen and natural gas have different combustion characteristics, it was fitted with a flashback-proof burner, suitable for firing all grades of fuel.

The burner, Figure 4.1, has two separate fuel gas feed systems that allow the simultaneous or alternate combustion of different fuel gases. The first gas (hydrogen or natural gas) is evenly distributed through the inner air annulus ring (1), while the second is distributed through the outer register ring (2) and discharged through the gas outlet

holes (3) into a region of high air velocity in the combustion air annulus (4). Thus, an intensive and homogenous mixing of gas and combustion air is achieved, which is then ignited by a gas-electric igniter located in the oval tube for the igniter and flame scanner (5).

The combustion air is supplied by a fan and evenly conducted through the windbox (6) and combustion air annulus (4) into the flame; additionally, through the inner air connection (7), air is conducted into the flame core, which, together with flue gas recirculation (FGR), has the effect of reducing the peak flame temperature and the formation of nitrogen oxides.

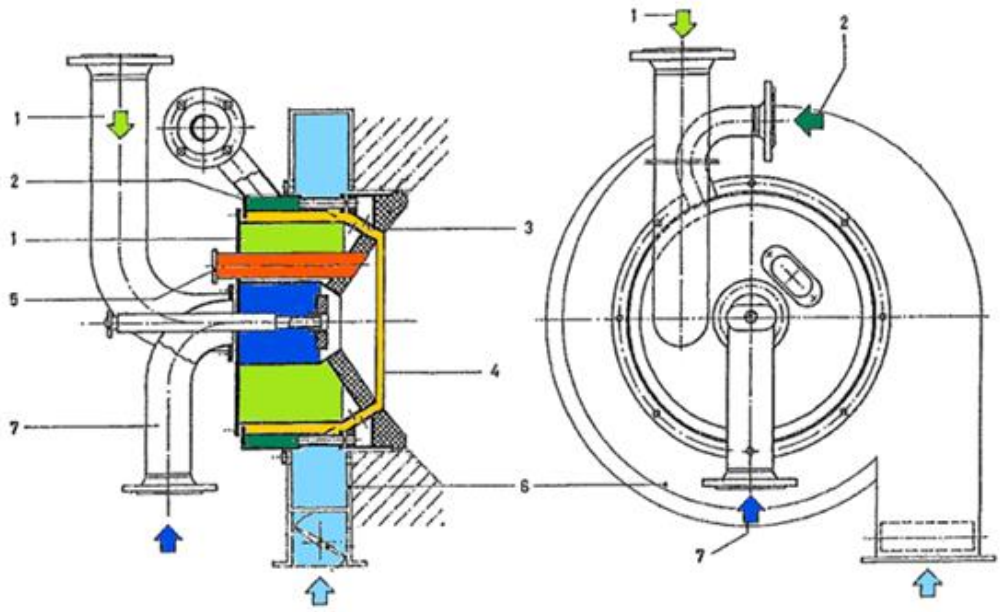

(1) – Inner air annulus ring
(2) – Outer register ring
(3) – Gas outlet holes
(4) – Combustion air annulus
(5) – Oval tube for igniter and flame scanner
(6) – Windbox
(7) – Inner air connection

Figure 4.1 – Register type Burner [66]

4.3. Flue Gas Analysis

The exhaust gas analysis was carried out using a sampling point in the exhaust funnel, Figure 4.2, located after the economizer, 2.7 metre above the exhaust outlet, and 19 metre below the top of the funnel.

Figure 4.2 – Exhaust Funnel

Figure 4.3 - Data Collection Set-Up

The emission analysis was carried out using a Testo 350 Flue Gas Analyzer installed with six different sensors that allowed for the measurement of CO, CO_2, NO, NO_2, SO_2, H_2S, and C_xH_y, and an industrial probe set, enabling the extractive sampling of flue gas at high temperatures (up to 1200ºC). The data relevant to the analyzer measuring range, accuracy and resolution can be found in the Annex A – Technical data Testo 350. The test data was directly downloaded to a laptop, Figure 4.3, and later the data regarding the amounts of CO_2, NO, and NO_2 present in the flue gas were analysed and discussed.

Data regarding fuel volumetric flows ($\dot{V}$) collected at the time of the tests, together with density (ρ) and gravimetric energy densities (G), were utilised in Equations (3), (4), and (5) to calculate the percentage of the energetic contribution of each fuel present during each test time.

$$\dot{V} \cdot \rho = \dot{m} \tag{3}$$

$$\dot{m} \cdot G = P \tag{4}$$

$$P_T = P_{GN} + P_{H2} \tag{5}$$

4.4. Combustion Process Simulation

To execute a model of the combustion reaction occurring in the boiler, chemical kinetics simulation software, ANSYS Chemkin, was used in parallel with GRI-Mech, which is an optimised chemical reaction mechanism for the calculation of natural gas and hydrogen chemical reaction processes. Its latest version, the GRI 3.0 mechanism [84], includes a detailed set of chemical reactions and species that describe how different chemical species react with each other during combustion. The mechanism is crucial for accurately capturing the combustion process and it was chosen since it has been validated by large experimental data for methane, ethane, carbon monoxide, and hydrogen.

Using the simulation software, the values for the adiabatic flame temperature were achieved for five working conditions: 100% natural gas, 100% hydrogen, and three blends of both with different ratios. While the values for the flame speed were only simulated for three working conditions.

The natural gas composition chosen is presented in Table 4.1, the values were based on information published by Portgás, a major natural gas distributor in Portugal [85].

Table 4.1 – Natural Gas composition

		Fuel Fraction of Total Fuel Species
Species (mole)		
Methane	CH4	0.9
Ethane	C2H6	0.07
Propane	C3H8	0.017
Carbon Dioxide	CO2	0.007
Nitrogen gas	N2	0.006

$$(\alpha C_x \mathrm{H_y} + \beta H_2) + (2\alpha + \frac{\beta}{2}) \cdot (O_2 + 3.76 N_2) = \alpha CO_2 + (2\alpha + \beta) \cdot H_2O + (2\alpha + \frac{\beta}{2}) \cdot 3.76 \cdot N_2 \quad (2)$$

The compositions of the hydrogen and natural gas mixtures were determined using Equation (2), where the number of carbon atoms present in the reaction decreases as hydrogen (β) replaces hydrocarbons (α) in the fuel composition. The composition of all the mixtures used in the simulations is set out in Table 4.2.

Table 4.2 – Simulated mixtures compositions

		Percentage of Hydrogen in the mixture				
		0%	25%	50%	75%	100%
Species (mole)						
Hydrogen	H2	0	0.25	0.5	0.75	1
Methane	CH4	0.9	0.675	0.45	0.225	0
Ethane	C2H6	0.07	0.0525	0.035	0.0175	0
Propane	C3H8	0.017	0.01275	0.0085	0.00425	0
Carbon Dioxide	CO2	0.007	0.00525	0.0035	0.00175	0
Nitrogen gas	N2	0.006	0.0045	0.003	0.0015	0

4.4.1. Adiabatic Flame Temperature

The adiabatic flame temperature simulation model uses a single equilibrium reactor at constant pressure and enthalpy together with GRI 3.0, which consists of 325 chemical reactions and thermochemical parameters for 53 species. The parameters used for the simulations are shown in Figure 4.4.

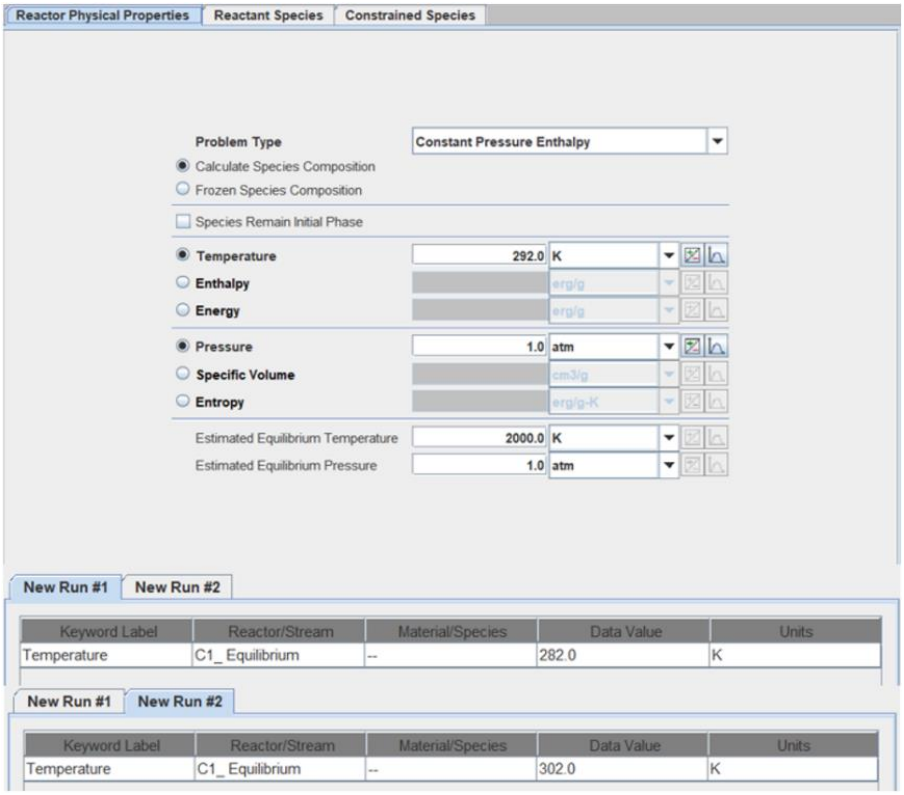

Figure 4.4 - Chemkin | Adiabatic Flame Temperature | Reactor Physical Properties

The initial temperature was set at 292 K, the pressure was set at 1 atm, and the estimated solution temperature was set at 2000 K, to help ensure that the solution obtained is for an ignited gas rather than an unburned state. Moreover, two additional runs were executed with the initial temperatures of 10 °C (282 K) and 30 °C (302 K).

4.4.2. Flame Speed

To predict the values of the laminar flame speed of natural gas-air, hydrogen-air, and a blend of both with air mixtures, the Flame Speed simulation in ANSYS Chemkin was used together with the chemical kinetics mechanism, GRI 3.0. The reacting flow model was set up to represent the conditions of a premixed flame, where the reactants are perfectly mixed before combustion.

The initial conditions were set to 292 K at atmospheric pressure, with a freely propagating flame and an automatic estimated temperature profile, Figure 4.5. Additionally, the simulations were done with the fuel mixtures, as in Table 4.2, and over a range of equivalence ratios, 0.6–1.4, allowing the comparison of the flame speed in fuel-lean and fuel-rich systems.

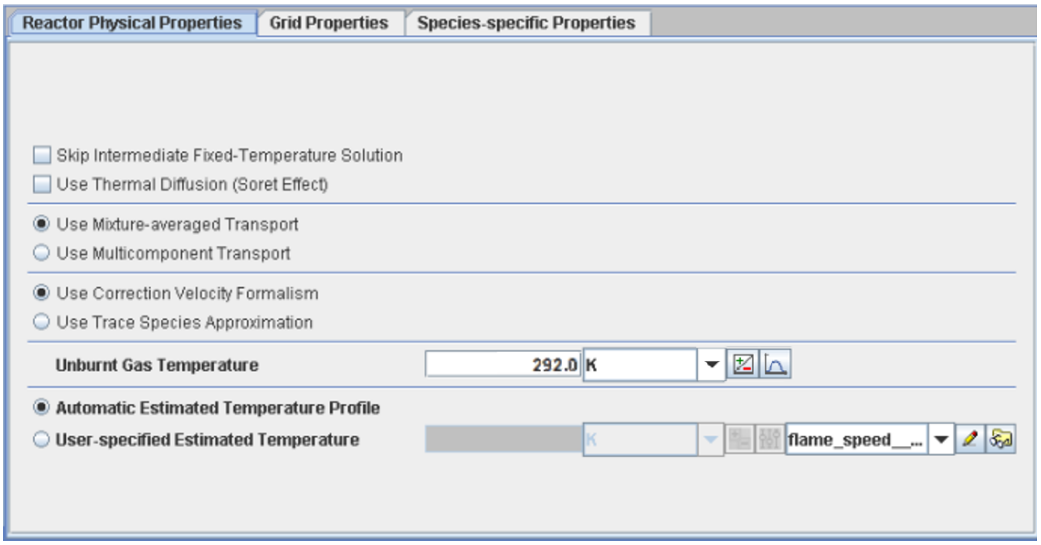

Figure 4.5 – Chemkin | Flame Speed | Reactor Physical Properties

The Flame Speed simulation uses computational fluid dynamics (CFD) techniques to model the flow field and combustion reactions. As the simulation progresses, a flame front forms and propagates through the mixture. The flame front is the region where

combustion reactions occur, and it separates the unburned mixture from the burned products. Throughout the simulation, the software tracks the concentrations of different chemical species and the temperature within the reacting flow domain. After the simulation is complete, visualisation tools help in interpreting the spatial distribution of temperature, species concentrations, and other relevant parameters [86].

To ensure that the gradients of gas temperature and major species were nearly zero at both boundaries, so that the requirements of adiabatic and zero-diffusive-flux conditions at the boundaries were met, the simulation was started on a small domain and unrefined grid and subsequently used Continuations to expand the domain and refine the grid. A starting small domain of 0.3 cm was specified in the Grid Properties panel, Figure 4.6. Subsequently, in the Continuations panel, the domain was expanded to 12 cm. (the starting axial position was expanded to -2 cm and the ending axial position to 10 cm).

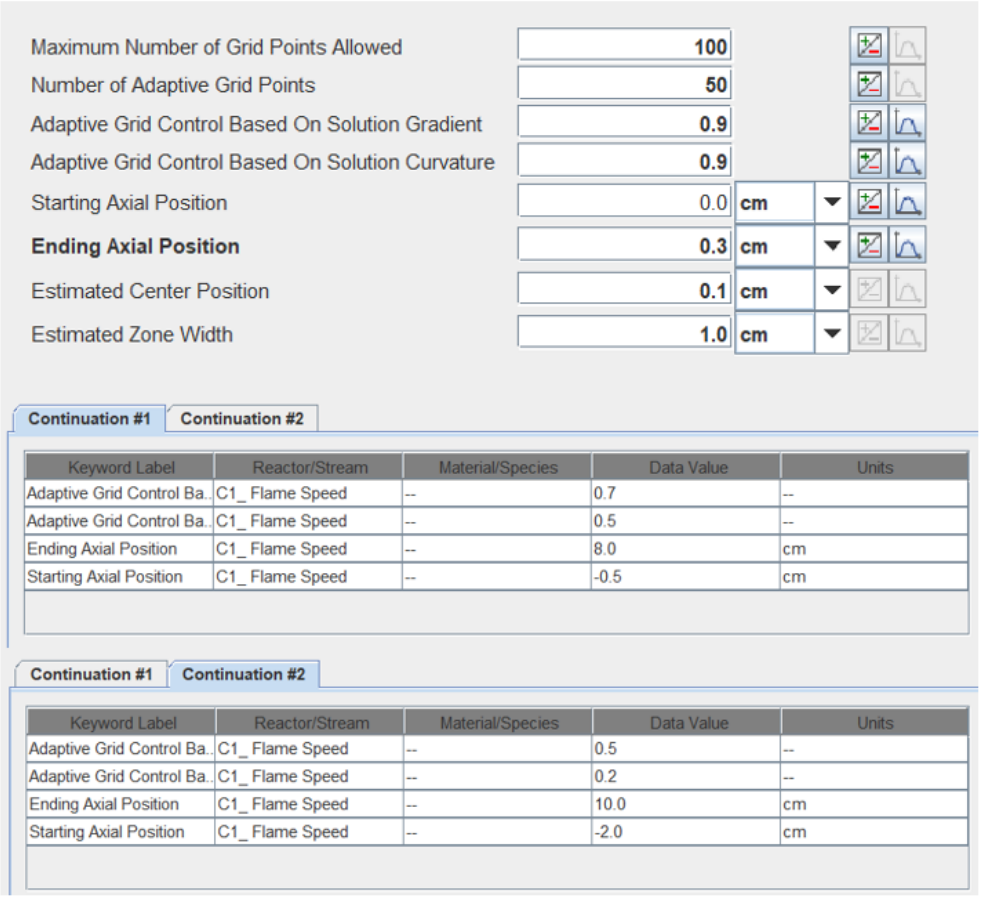

Figure 4.6 – Chemkin | Flame Speed | Grid Properties

The model uses a non-uniform grid that is successively and automatically adapted based on solution gradients and curvatures determined on an initially coarse grid. Relative gradient and curvature parameters that determine the extent to which the solution will be refined were model inputs. The relative gradient and curvature parameters for the grid refinement were both set in the Grid Properties panel to 0.9. Subsequently, in the Continuations panel, these values are both lowered to 0.2, to obtain a finer grid. To allow sufficient grid points for a well refined grid, the maximum number of grid points was set to 100.

Even though the simulation results are often compared with experimental data to validate the accuracy of the chemical kinetics mechanism and the numerical model, it was not possible to execute such a comparison since there was no experimental data to compare with.

5. Results

5.1. Adiabatic Flame Temperature

The adiabatic flame temperature of a mixture is the temperature it will reach when burning under ideal conditions. However, in a real system, heat losses and incomplete combustion mean the combustion temperature will not reach the adiabatic temperature. Using Chemkin, the adiabatic flame temperature can be reached by simulating the combustion in constant volume or constant pressure conditions; the latter was chosen for the model tests, because 1 atmosphere is the value for the pressure. Moreover, the test was executed with an initial temperature of 20 °C (292 K) and two additional runs for the temperatures of 10 °C (282 K) and 30 °C (302 K).

The simulation was executed for the combustion of 100% natural gas and 100% hydrogen. As the results expressed in Table 5.1 show, the values obtained are within the range of the values found in the literature, Table 3.2.

Table 5.1 – Natural Gas and Hydrogen Equilibrium Temperature

Equilibrium Temperature (K)	
Natural Gas	2225
Hydrogen	2377

Additional simulations were performed using various natural gas and hydrogen mixtures (Table 4.2), the results of the five runs for each Chemkin simulation, in Figure 5.1, displayed in equilibrium temperature vs initial temperature, similarity, show that the effect the initial temperature has on the adiabatic flame temperature is independent from the hydrogen quantity in the mixture.

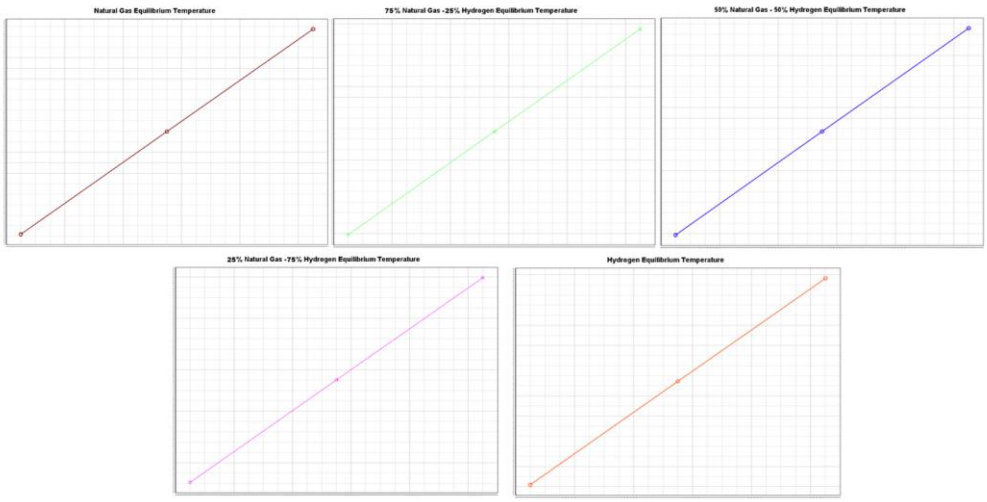

Figure 5.1 – Adiabatic Flame Temperature | Simulations Nº1-5 | Results plotted

The results of the adiabatic flame temperature for the initial temperature of 292 K were grouped and are plotted in Figure 5.2, where it is possible to conclude that the temperature does not increase linearly, having a greater increase as the hydrogen percentage increases. Due to the increased flame temperature of hydrogen, the thermal capacity of the materials used in natural gas burners, such as the nozzle, flame stabiliser, and refractory throat, require a review, whether they are metallic or ceramic.

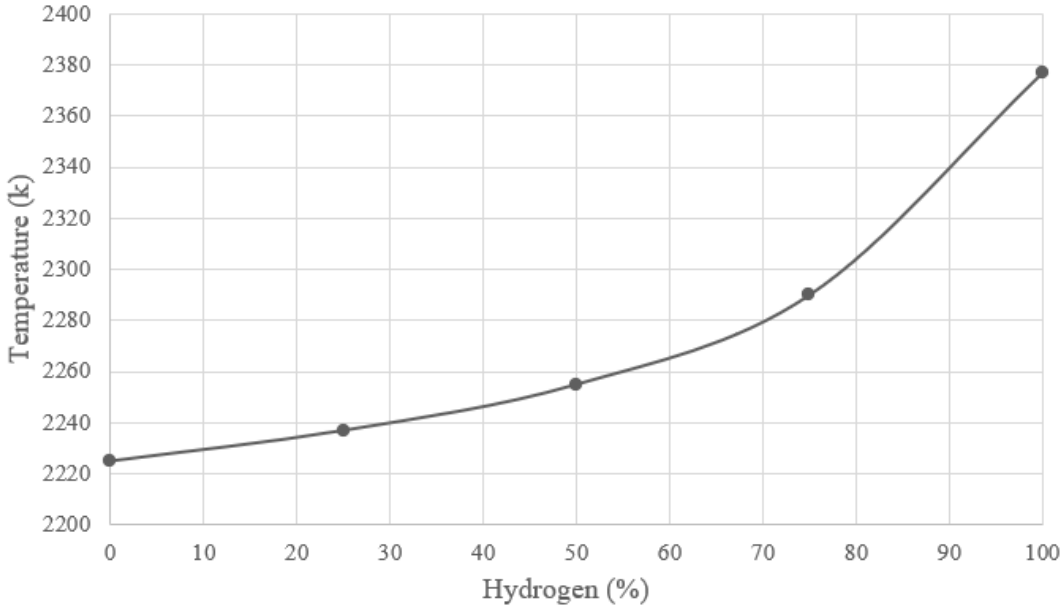

Figure 5.2 – Adiabatic Flame Temperature

When choosing gas burner materials, phenomena such as hydrogen embrittlement and high-temperature hydrogen attack should be taken into consideration, as these effects can lead to premature degradation and failure of the burner parts [72].

5.2. Flame Speed

After running the simulations with three different fuel mixtures (Table 4.2), the results of the runs for each Chemkin simulation in Figure 5.3, are displayed similarity in flame speed (cm/s) vs equivalence ratio.

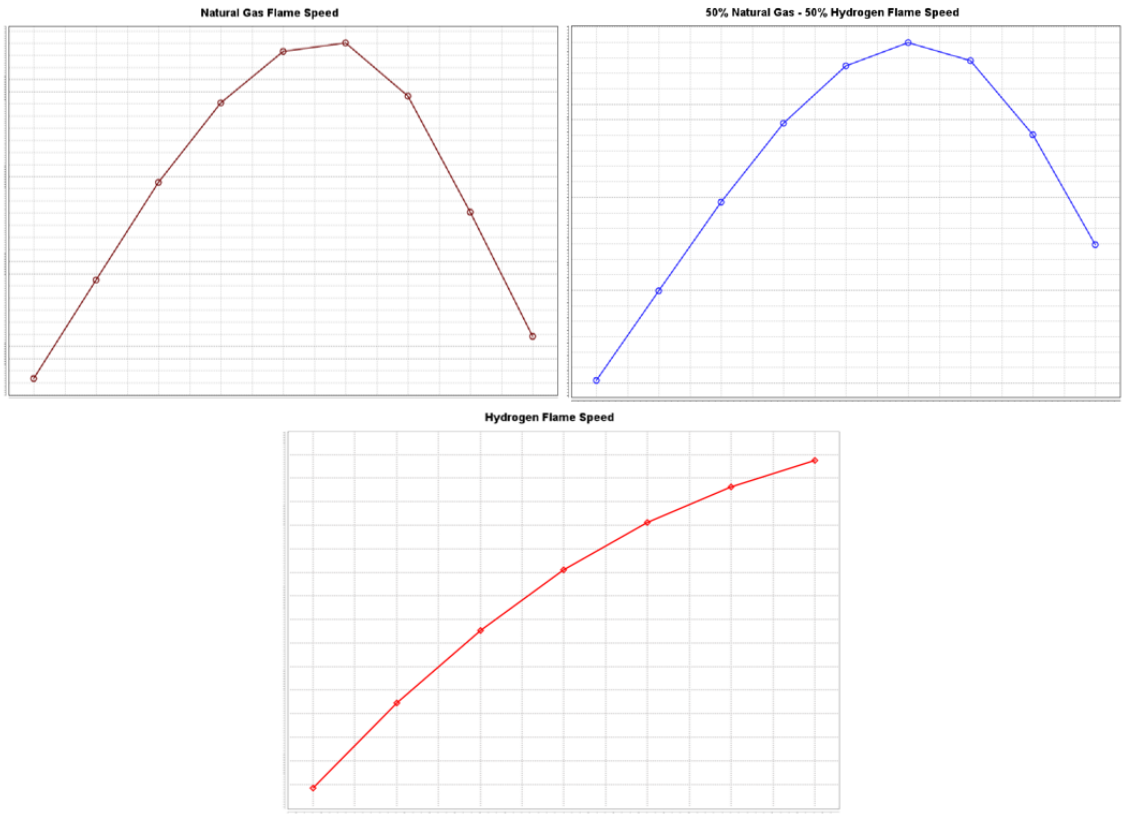

Figure 5.3 – Flame Speed | Simulations Nº1,3 and 5 | Results plotted

The data from the plotted graphs was grouped and the results obtained, displayed in Figure 5.4. It is possible to ascertain that the increase in the flame speed is not linear and that it is greater the higher the percentage of hydrogen.

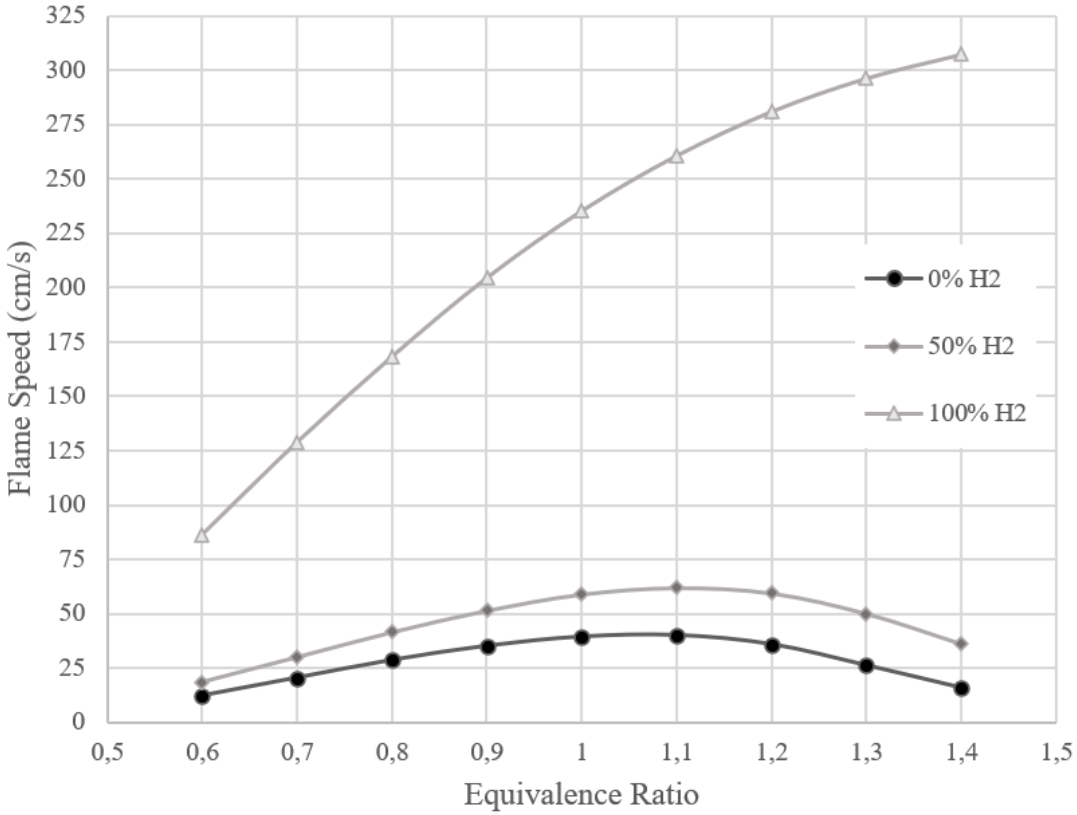

Figure 5.4 – Flame Speed vs Equivalence Ratio

The fuel's flame speed increases with the presence of hydrogen. With stoichiometric conditions, the natural gas flame speed is 40 cm/s, while for the 50/50 blend of both fuels, it is 59 cm/s. When hydrogen makes up the totality of the fuel, the flame speed is 235 cm/s.

5.3. Nitrogen and carbon oxides emissions

The effect of burner emissions is a crucial matter when considering H_2 firing. As compared to natural gas, hydrogen's high flame propagation speed leads to quicker combustion with a more intense energy release on a small area; moreover, the localised elevation of near-flame temperatures caused by this quick combustion process amplifies the influence of the high flame temperatures on NO_x emission rates.

Any area with temperatures above 1371 °C is favourable for NO_x formation, and, to avoid such a phenomenon, the different approaches that can be taken typically include flue gas recirculation (FGR), steam injection, or ultra-low-NOx burner technologies (ULN).

Flue gas recirculation consists of using a portion of the boiler exhaust gases into the combustion air supply, diluting the combustion air supply with spent combustion products; consequently, during combustion, the peak flame temperature is lowered. Small amounts of carefully placed steam injections have the effect of cooling the flame and inerting a small amount of the mixture. Staged ULN burners commonly use air and fuel staging to decrease peak flame temperature. A properly staged fuel increases the amount of furnace gas entrained into the fuel stream prior to interacting with the air, having a similar effect to the FGR regarding NOx mitigation. Additionally, properly staged air within the combustion zone delays the mixing of the fuel and air, stretching the combustion process over the length of the furnace. The extended combustion process decreases overall peak combustion temperatures [72].

The exhaust gas analysis results of HyChem's boiler are shown in Table 5.2. In an uncontrolled combustion, it is expected that the amount of nitrogen oxides emitted by the hydrogen combustion should be higher, but since the boiler has NOx reduction features such as flue gas recirculation and staged air intake, the emissions from natural gas and hydrogen combustion are similar, as seen in Table 5.2. The results show a slight increase in the presence of nitrogen oxides in the blends, and that is due to inaccurate calibration of the air staging and flue gas recirculation for blended mixtures.

Table 5.2 – Nitrogen Oxides Quantities

	NO (ppm)	NO2 (ppm)	NOx (ppm)
H2 (%)			
0	34	5.1	39.1
65.4	48	5.2	53.2
71.7	57	5.3	62.3
73.5	59	5.7	64.7
100	36	3.5	39.5

The amount of H_2 in the fuel has a significant impact on CO_2 emissions. From Equation (2), it is possible to ascertain that the number of carbon atoms present decreases as hydrogen (β) replaces hydrocarbons (α) in the fuel composition. Due to the lack of carbon in the combustion reaction, a fuel stream composed entirely of H_2 produces residual amounts to none of CO_2 as a by-product of combustion, being lubricants and impurities in the stream, the origin of the residual amounts of carbon.

As a result, and as evidenced by the data in Figure 5.5, collected in the exhaust gas analysis, the increasing amount of hydrogen in the fuel mixture results in a nonlinear reduction in CO_2 emissions. The reduction in CO_2 emissions is greater, the higher the amount of hydrogen present in the mixture.

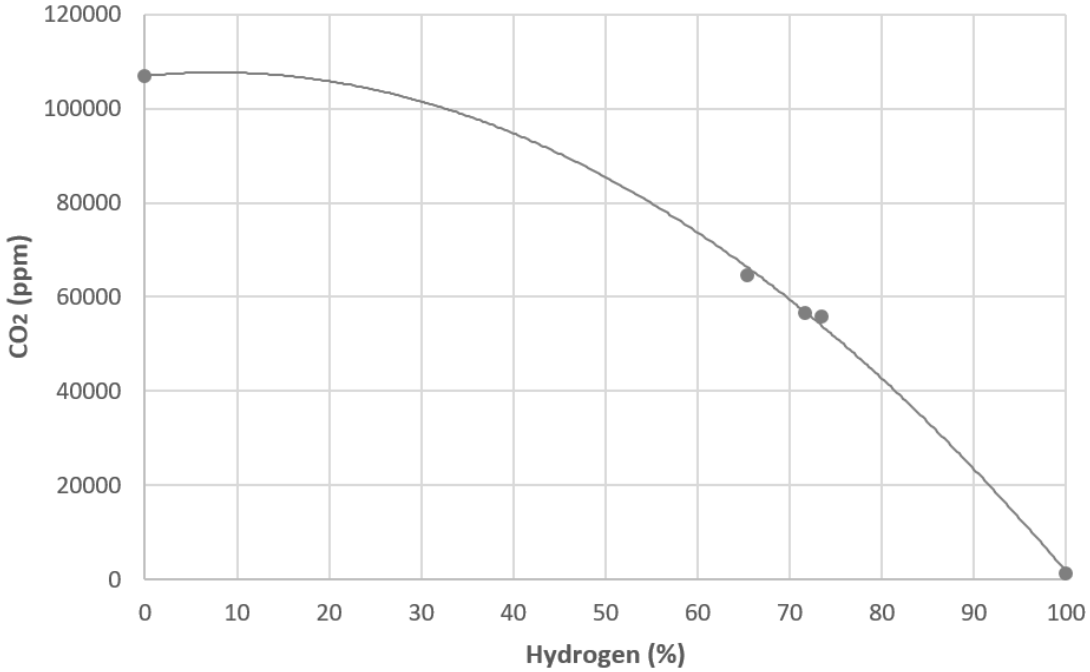

Figure 5.5 – Carbon Dioxide Quantities

The results show that when burning only natural gas, 10.7% of the exhaust gases are CO_2. When the fuel blend was composed of about 35% natural gas and 65% hydrogen, the percentage of CO_2 was 6.5%, representing a 39% reduction in CO_2 emissions. With 72% and 74% hydrogen in the blend, the CO_2 present in the exhaust gases is 5.7% and 5.6%, respectively, representing a reduction of 47% and 48% in carbon dioxide emissions when compared with burning natural gas. While running only on hydrogen, 0.13% of the exhaust gas was relative to CO_2, which represented a 98.8% reduction when compared with burning natural gas.

Even though theoretically there were no hydrocarbons present in the fuel mixture the carbon present in the flue gas can be justified by the presence of carbon impurities remaining from the electrolysis process.

6. Conclusions and Future Works

6.1. Conclusions

The acceptance of hydrogen as a net zero fuel is increasing, and it will undoubtedly play a significant role in future energy systems for storage, transmission, and achieving decarbonization goals. The transition from fossil fuels to carbon-free solutions requires no re-invention of industrial processes, and HyChem is an example of how the simplicity and relatively minor technical changes required to burn hydrogen mean that this path will almost certainly be followed in many industries, alongside other approaches such as fuel cells.

The exhaust gas analysis showed that the addition of hydrogen to a natural gas-fuelled boiler allowed for a reduction in carbon dioxide emissions, with the reduction being higher with the increase in the amount of hydrogen in the fuel mixture, owing to the boiler being prepared to burn both fuel grades. As seen, when hydrogen is burned the high flame speed increases the susceptibility of the occurrence of flashback, however by using flashback-proof technology burners and/or running the boiler on lean hydrogen mixtures this problem can be minimized. In addition, if the high adiabatic temperature of hydrogen is not addressed, the formation of nitrogen oxide emissions will occur, however if combustion equipment's comprise low NOx technologies, these emissions will not worsen with widespread adoption. Other air pollutant emissions from hydrogen are environmentally better than fossil fuel equivalents, such as carbon dioxide or directly emitted specific matter, and these advantages must be considered in cost-benefit assessments.

Ships vary in size and function, their power demand, space available and fuel autonomy differ from sector to sector. While deep-sea going cargo vessels, such as container and bulk carriers, have large power demands and require big fuel amounts, short-sea and inland waterways vessels, such as ferries and tugs, do not require big amounts of power or autonomy. Moreover, sailing some areas of the globe creates constraints regarding fuel emissions. That being said, it is likely that each sector will use the hydrogen technology that suits its demands better. As for now, hydrogen is currently concentrated in short-sea and short applications in Emission Control Areas, as well as auxiliary engines and hotel load. However, hydrogen use in combustion engines is a

reality in dual-fuel engines, with some manufacturers already offering IMO Tier III compliant engines.

In summary, hydrogen as an energy source is a viable solution to reduce some environmentally harmful emissions and although some of its technologies are far from reaching maturity it is a suitable solution for some applications including some sectors of the maritime trade. One key advantage of some hydrogen combustion technologies is that they do not require major changes in the infrastructure, production chains are already existent, and they have a long lifespan. While transportation and storage are still constraining in the hydrogen supply chain, industries close to green or pink hydrogen production sources will not have to deal with those problems.

6.2. Future Works

Some future work suggestions can now be made considering the conclusions.

First, an overview of existent local legislation regarding emissions can be carried out to assess how it can impact existent industries and their infrastructure soon depending on their location.

A complete study regarding the economic viability of using hydrogen can be carried out by assessing the costs related not only to the retrofitted boiler but also to the adjacent infrastructure, hydrogen production and transport, and maintenance operations.

Lastly, a more detailed overview of technology ready to be used onboard could also be of interest.

References

[1] United States Environmental Protection Agency, “Overview of Greenhouse Gases,” 12 10 2021. [Online]. Available: https://www.epa.gov/ghgemissions/overview-greenhouse-gases. [Accessed 17 11 2021].

[2] International Maritime Organization, “Greenhouse Gas Emissions,” 2020. [Online]. Available: https://www.imo.org/en/OurWork/Environment/Pages/GHG-Emissions.aspx. [Accessed 03 01 2021].

[3] N. Rehmatulla, J. Calleya and T. Smith, “The implementation of technical energy efficiency and CO2 emission reduction measures in shipping,” 2017. [Online]. Available: https://www.sciencedirect.com/science/article/pii/S0029801817302160. [Accessed 04 01 2021].

[4] H. Ritchie and M. Roser, “CO_2 and Greenhouse Gas Emissions,” OurWorldInData.org, 2020. [Online]. Available: https://ourworldindata.org/co2-and-other-greenhouse-gas-emissions. [Accessed 21 11 2021].

[5] M. Cames, J. Graichen, A. Siemons and V. Cook, “Emission reduction targets for international aviation and shipping,” 2015. [Online]. Available: http://www.europarl.europa.eu/RegData/etudes/STUD/2015/569964/IPOL_STU(2015)569964_EN.pdf.

[6] International Chamber of Shipping, “International Chamber of Shipping sets out plans for global carbon levy to expedite industry decarbonisation,” 06 09 2021. [Online]. Available: https://www.ics-shipping.org/press-release/international-chamber-of-shipping-sets-out-plans-for-global-carbon-levy/. [Accessed 16 11 2021].

[7] CMA CGM, “The CMA CGM JACQUES SAADE, the world's first 23,000 TEU powered by LNG,” 13 11 2020. [Online]. Available: https://cmacgm-group.com/en/launching-cmacgm-jacques-saad%C3%A9-world's-first-ultra-large-vessel-powered-by-lng. [Accessed 04 01 2021].

[8] M. Placek, “Age distribution of the world merchant fleet in 2019-2020, by vessel type,” Statista, 05 10 2021. [Online]. Available: https://www.statista.com/statistics/1102442/age-of-world-merchant-fleet-by-vessel-type/. [Accessed 28 11 2021].

[9] J. B. Cristello, J. M. Yang, R. Hugo, Y. Lee and S. S. Park, “Feasibility analysis of blending hydrogen into natural gas networks,” *International Journal of Hydrogen Energy,* vol. 48, no. 46, pp. 17605-17629, 2023.

[10] X. Tian and J. Pei, “Study progress on the pipeline transportation safety of hydrogen-blended natural gas,” *Heliyon,* vol. 9, no. 11, 2023.

[11] Y.-Q. Zhu, W. Song, H.-B. Wang, J.-T. Qi, R.-C. Zeng, H. Ren, W.-C. Jiang, H.-B. Meng and Y.-X. Li, “Advances in reducing hydrogen effect of pipeline steels on hydrogen-blended natural gas transportation: A systematic review of

mitigation strategies," *Renewable and Sustainable Energy Reviews,* vol. 189, 2024.

[12] F. Sorgulu and I. Dincer, "Analysis and techno-economic assessment of renewable hydrogen production and blending into natural gas for better sustainability," *International Journal of Hydrogen Energy,* vol. 47, no. 46, pp. 19977-19988, 2022.

[13] S. Bellocchi, M. D. Falco, M. Facchino and M. Manno, "Hydrogen blending in Italian natural gas grid: Scenario analysis and LCA," *Journal of Cleaner Production,* vol. 416, 2023.

[14] M. Ozturk, F. Sorgulu, N. Javani and I. Dincer, "An experimental study on the environmental impact of hydrogen and natural gas blend burning," *Chemosphere,* vol. 329, 2023.

[15] F. Sorgulu, M. Ozturk, N. Javani and I. Dincer, "Experimental investigation for combustion performance of hydrogen and natural gas fuel blends," *International Journal of Hydrogen Energy,* vol. 48, no. 88, pp. 34476-34485, 2023.

[16] J. Babicz, "Encyclopedia of Ship Technology," Wärtsilä Corporation, 2015.

[17] J. Trindade, "Motores de Combustão Interna," ENIDH, 2014.

[18] MAN Energy Solutions, "Hydrogen in shipping," Augsburg, Germany, 2021.

[19] Pacific Northwest National Laboratory, "Hydrogen Tools," U.S. Department of Energy's Office of Energy Efficiency and Renewable Energy, [Online]. Available: https://h2tools.org/hyarc/hydrogen-data/basic-hydrogen-properties. [Accessed 19 12 2021].

[20] Engineering ToolBox, "Fuels - Densities and Specific Volumes," 2003. [Online]. Available: https://www.engineeringtoolbox.com/fuels-densities-specific-volumes-d_166.html. [Accessed 19 12 2021].

[21] Shell Deutschland Oil GmbH, "SHELL Hydrogen Study: Energy of the future," *Sustainable Mobility through Fuel Cells and H2,* 2020.

[22] N. Rusman and M. Dahari, "A review on the current progress of metal hydrides material for solid-state hydrogen storage applications," *International Journal of Hydrogen Energy,* vol. 41, no. 28, 2016.

[23] R. Moradi and K. M. Groth, "Hydrogen storage and delivery: Review of the state of the art technologies and risk and reliability analysis," *International Journal of Hydrogen Energy,* vol. 44, no. 23, pp. 12254-12269, 2019.

[24] W. L. Jolly, "Hydrogen," Encyclopedia Britannica, 01 June 2020. [Online]. Available: https://www.britannica.com/science/hydrogen. [Accessed 05 01 2022].

[25] C. H. Holbrow and J. C. Amato, "Gay-Lussac Did Better Than He Knew," *Joint Spring 2011 Meeting of the New England Sections of the APS and the AAPT,* 8-9 04 2011.

[26] J. Wilken, "System Study of Slush Propellants for Future European Launch Vehicles.," in *Space Propulsion ,* Seville, 2018.

[27] National Grid, “The hydrogen colour spectrum,” National Grid, 2022. [Online]. Available: https://www.nationalgrid.com/stories/energy-explained/hydrogen-colour-spectrum. [Accessed 11 01 2022].

[28] S. A and Y. Shabong, “BP plans large-scale green hydrogen project in UK,” Reuters, Bengaluru, 2021.

[29] Iberdrola, “Iberdrola builds the largest green hydrogen plant for industrial use in Europe,” 2021.

[30] M. B. Powers, “Green Hydrogen Plants Scale Up in North America,” Engineering News-Record, 2021.

[31] L. Bertuccioli, A. Chan, D. Hart, F. Lehner, B. Madden and E. Standen, “Study on development of water electrolysis in the EU,” 2014.

[32] A. Arregi, M. Amutio, G. Lopez, J. Bilbao and M. Olazar, “Evaluation of thermochemical routes for hydrogen production from biomass: A review,” *Energy Conversion and Management,* vol. 165, pp. 696-719, 2018.

[33] R. Kothari, D. Buddhi and R. Sawhney, “Comparison of environmental and economic aspects of various hydrogen production methods,” *Renewable and Sustainable Energy Reviews,* vol. 12, no. 2, pp. 553-563, 2008.

[34] M. El-Shafie, S. Kambara and Y. Hayakawa, “Hydrogen Production Technologies Overview,” *Journal of Power and Energy Engineering,* vol. 7, no. 1 (2019), p. 48, 2019.

[35] L. v. Biert, M. Godjevac, K. Visser and P. Aravind, “A review of fuel cell systems for maritime applications,” *Journal of Power Sources,* pp. 345-364, 2016.

[36] J. Chi and H. Yu, “Water electrolysis based on renewable energy for hydrogen production,” *Chinese Journal of Catalysis,* vol. 396, no. 3, pp. 390-394, 2018.

[37] H. Xing, C. Stuart, S. Spence and H. Chen, “Fuel Cell Power Systems for Maritime Applications: Progress and Perspectives,” *Sustainability,* vol. 1213, no. 13, 2021.

[38] International Energy Agency, “The future of Hydrogen,” IEA Publications, Paris, 2019.

[39] R. Rosli, A. Sulong, W. Daud, M. Zulkifley, T. Husaini, M. Rosli, E. Majlan and M. Haque, “A review of high-temperature proton exchange membrane fuel cell (HT-PEMFC) system.,” *Journal of Hydrogen Energy,* vol. 42, p. 9293–9314, 2017.

[40] T. Tronstad, H. Åstrand, G. Haugom and L. Langfeldt, “Study on the Use of Fuel cells in Shipping;,” DNV GL, Oslo, Norway, 2017.

[41] W. Dai, H. Wang, X. Yuan, J. Martin, D. Yang, J. Qiao and J. Ma, “A review on water balance in the membrane electrode assembly of proton exchange membrane fuel cells.,” *Journal of Hydrogen Energy,* vol. 34, p. 9461–9478, 2009.

[42] Inland Transport Committee, “Request for a recommendation on the use of hydrogen fuel cells for the propulsion of the vessel "FPS Waal",” Geneva, 2023.

[43] Ballard, “Ballard fuel cells installed onboard the world’s first liquid hydrogen-powered ferry,” 2022.

[44] FuelCellsWorks, “ELEKTRA Hydrogen Fuel Cell/Baterry Hybrid Push Boat in Service,” 2021.

[45] Fastech, “The Past, Present and Future of Hydrogen Vehicles: 2023 Update,” 2023.

[46] O. A. a. M. P. M. W. Melaina, “Blending Hydrogen into Natural Gas Pipeline Networks: A Review of Key Issues,” Colorado, 2013.

[47] J. Guarco, B. Langstine and M. Turner, “Practical considerations for firing hydrogen versus natural gas,” [Online]. Available: https://cea.org.uk/practical-considerations-for-firing-hydrogen-versus-natural-gas/. [Accessed 04 2023].

[48] A. Helmenstine, “Science Notes,” 06 01 2021. [Online]. Available: https://sciencenotes.org/adiabatic-flame-temperature-chart/.

[49] Engineering Toolbox, “Adiabatic Flame Temperatures,” 2005.

[50] Princeton University, “Thermodynamic Glossary - Adiabatic Flame Temperature”.

[51] P. A. M. Helmenstine, “Flame Temperatures Table for Different Fuels,” 2020.

[52] A. Lanz, J. Heffel and C. Messer, “Hydrogen Fuel Cell Engines and Related Technologies,” 2001.

[53] M. O. V.-M. A. S. N. &. D. l. R.-U. D. Vigueras-Zúñiga, “Flashback Avoidance in Swirling Flow Burners,” *Ingeniería, investigación y tecnología,* vol. 15, no. 4, pp. 603-614, 2014.

[54] A. Boretti, “Hydrogen internal combustion engines to 2030,” Elsevier Ltd., Saudi Arabia, 2020.

[55] Toyota Motor Corp., “Toyota Developing Hydrogen Engine Technologies Through Motorsports,” Toyota City, Japan, 2021.

[56] CMB.TECH, “Hydrocat Powered by Hydrogen,” Antwerp, 2023.

[57] The Japan Times, “In defense of combustion engines, Toyota CEO says ‘the enemy is carbon’,” Tokyo, 2021.

[58] International Maritime Organization (IMO), “International Maritime Organization,” [Online]. Available: https://www.imo.org/.

[59] International Maritime Organization, “Conventions,” [Online]. Available: https://www.imo.org/en/About/Conventions/Pages/Default.aspx.

[60] International Maritime Organization, “International Convention for the Prevention of Pollution from Ships (MARPOL),” [Online]. Available: https://www.imo.org/en/about/Conventions/Pages/International-Convention-for-the-Prevention-of-Pollution-from-Ships-(MARPOL).aspx.

[61] United States Environmental Protection Agency, “MARPOL Annex VI and the Act To Prevent Pollution From Ships (APPS),” [Online]. Available: https://www.epa.gov/enforcement/marpol-annex-vi-and-act-prevent-pollution-ships-apps.

[62] United States Environmental Protection Agency, “Particulate Matter (PM) Pollution,” 2023.

[63] S. Ahmed and X.-C. Gu, “Accident-based FMECA study of Marine boiler for risk prioritization using fuzzy expert system,” *Results in Engineering,* vol. 6, 2020.

[64] INDUSTRIAL BOILER & MECHANICAL, “Watertube boilers customized to your application.,” [Online]. Available: https://industrialboiler.com/boilers/watertube-boilers.

[65] INDUSTRIAL BOILER & MECHANICAL, “Industrial firetube boilers. An IB&M specialty.,” [Online]. Available: https://industrialboiler.com/boilers/firetube-boilers.

[66] H. SAACKE KG, “Register Type Burner for Two Fuel Gases,” Bremen, Germany, 1982.

[67] G. P. Smith, D. M. Golden, M. Frenklach, N. W. Moriarty, B. Eiteneer, M. Goldenberg, C. T. Bowman, R. K. Hanson, S. Song, W. C. G. Jr., V. V. Lissianski and Z. Qin, “GRI-Mech 3.0”.

[68] Portgás, “Composição do gás natural,” [Online]. Available: https://www.portgas.pt/profissionais/apoio/composicao-do-gas-natural/. [Accessed 15 01 2023].

[69] ANSYS, “ANSYS Chemkin Tutorials Manual,” ANSYS Reaction Design, San Diego, 2016.

[70] Testo, Flue gas analyzer for industry - Testo 350.

[71] I. Dincer and C. Acar, “Review and evaluation of hydrogen production,” *International Journal of Hydrogen Energy,* vol. 40, no. 34, pp. 11094-11111, 2015.

[72] A. Evans, V. Strezov and T. J. Evans, “Sustainability considerations for electricity generation from biomass,” *Renewable and Sustainable Energy Reviews,* vol. 5, no. 14, pp. 1419-1427, 2010.

[73] “The Fuel Cell Industry Review,” in *E4tech,* Lausanne/ London, 2016.

[74] C. J. Rhodes, “21 Best Diesel Marine Engines for Your Fishing Boat,” 2022.

7. Annexes

7.1. Annex A – Technical data Testo 350

7.1.1. Technical data Testo 350 analyzer box

	Measuring range	Accuracy ±1 digit	Resolution	Reaction time t_{90}
Degree of effectivity	0 to +120 %		0.1 % (0 to +120 %)	
Flue gas loss	0 to +99.9 % qA		0.1 % qA (-20 to +99.9 % qA)	
CO_2 calculation	0 to $CO_{2\,max}$ Vol. % CO_2	calculated from O_2 ±0.2 Vol.%	0.01 Vol. % CO_2	40 s
Differential pressure 1	-40 to +40 hPa	±1.5% of m.v. (-40 to -3 hPa) ±1.5% of m.v. (+3 to +40 hPa) ±0.03 hPa (-2.99 to +2.99 hPa)	0.01 hPa (-40 to +40 hPa)	
Differential pressure 2	-200 to +200 hPa	±1.5% of m.v. (-200 to -50 hPa) ±1.5% of m.v. (+50 to +200 hPa) ±0.5 hPa (-49.9 to +49.9 hPa)	0.1 hPa (-200 to +200 hPa)	
Flow velocity	0 to +40 m/s		0.1 m/s (0 to +40 m/s)	
Absolute pressure (opt. when equipped with IR sensor)	-600 to +1.150 hPa	±10 hPa	1 hPa	
Flue gas dewpoint calculation	0 to 99.9 °C td		0.1 °C td (0 to 99.9 °C td)	
Type K (NiCr-Ni)	-200 to +1.370 °C	±0.4 °C (-100 to +200 °C) ±1 °C (-200 to -100.1 °C) ±1 °C (+200.1 to +1370 °C)	0.1 °C (-200 to +1.370 °C)	
Type S (Pt10Rh-Pt)		±1 °C (0 to +1.760 °C)	0.1 °C (0 to +1.760 °C)	
Ambient temperature probe (NTC)	-20 to +50 °C	±0.2 °C (-10 to +50 °C)	0.1 °C (-20 to +50 °C)	
O_2 measurement	0 to +25 Vol. % O_2	±0.8% of fsv (0 to +25 Vol. % O_2)	0.01 Vol. % O_2 (0 to +25 Vol. % O_2)	20 s (t_{95})
CO measurement (H_2 compensated)*	0 to +10.000 ppm CO	±5% of m.v. (+200 to +2.000 ppm CO) ±10% of m.v. (+2.001 to +10.000 ppm CO) ±10 ppm CO (0 to +199 ppm CO)	1 ppm CO (0 to +10.000 ppm CO)	40 s
CO_{low} measurement (H_2 compensated)*	0 to 500 ppm CO	±5% of m.v. (+40 to +500 ppm CO) ±2% ppm CO (0 to +39,9 ppm CO)	0.1 ppm CO (0 to +500 ppm CO)	40 s
NO measurement	0 to +4.000 ppm NO	±5% of m.v. (+100 to +1.999 ppm NO) ±10% of m.v. (+2.000 to +4.000 ppm NO) ±5 ppm NO (0 to +99 ppm NO)	±1 ppm NO (0 to +4.000 ppm NO)	30 s
NO_{low} measurement	0 to +300 ppm NO	±5% of m.v. (+40 to +300 ppm NO) ±2 ppm NO (0 to +39.9 ppm NO)	±0.1 ppm NO (0 to +300 ppm NO)	30 s
NO_2 measurement	0 to +500 ppm NO_2	±5% of m.v. (+100 to +500 ppm NO_2) ±5 ppm NO_2 (0 to +99,9 ppm NO_2)	±0.1 ppm NO_2 (0 to +500 ppm NO_2)	40 s
SO_2 measurement	0 to +5.000 ppm SO_2	±5% of m.v. (+100 to +2.000 ppm SO_2) ±10% of m.v. (+2.001 to +5.000 ppm SO_2) ±5 ppm SO_2 (0 to +99 ppm SO_2)	±1 ppm SO_2 (0 to +5.000 ppm SO_2)	30 s
CO_2 measurement (IR)	0 to +50 Vol. % CO_2	±0.3 Vol. % CO_2 + 1% of m.v. (0 to 25 Vol. % CO_2) ±0.5 Vol. % CO_2 + 1.5% of m.v. (>25 to 50 Vol. % CO_2)	0.01 Vol. % CO_2 (0 to 25 Vol. % CO_2) 0.1 Vol. % CO_2 (>25 Vol. % CO_2)	10 s
H_2S measurement	0 to +300 ppm H_2S	±5% of m.v. (+40 to +300 ppm) ±2 ppm (0 to +39.9 ppm)	0.1 ppm (0 to +300 ppm)	35 s

* H_2 only as an indicator

Figure 7.1 - Testo 350 analyzer box technical data [70]

7.1.2. Technical data CxHy Sensor

Meas. parameter	Measuring range[1]	Accuracy ±1 digit	Resolution	Min. O_2 requirement in flue gas	Reaction time t_{90}	Response factor[2]
Methane	100 to 40.000 ppm	< 400 ppm (100 to 4.000 ppm) < 10% of m.v. (>4.000 ppm)	10 ppm	2% + (2 x m.v. methane)	< 40 s	1
Propane	100 to 21.000 ppm			2% + (5 x m.v. propane)		1.5
Butane	100 to 18.000 ppm			2% + (6.5 x m.v. butane)		2

[1] Lower explosion limit (LEL)must be adhered to.
[2] The HC sensor is adjusted to methane ex-works. It can be adjusted to a different gas (propane or butane) by the user.

Figure 7.2 - CxHy Sensor technical data [70]

7.2. Annex B - Adiabatic Flame Temperature Simulations

7.2.1. Adiabatic Flame Temperature Simulation Parameters

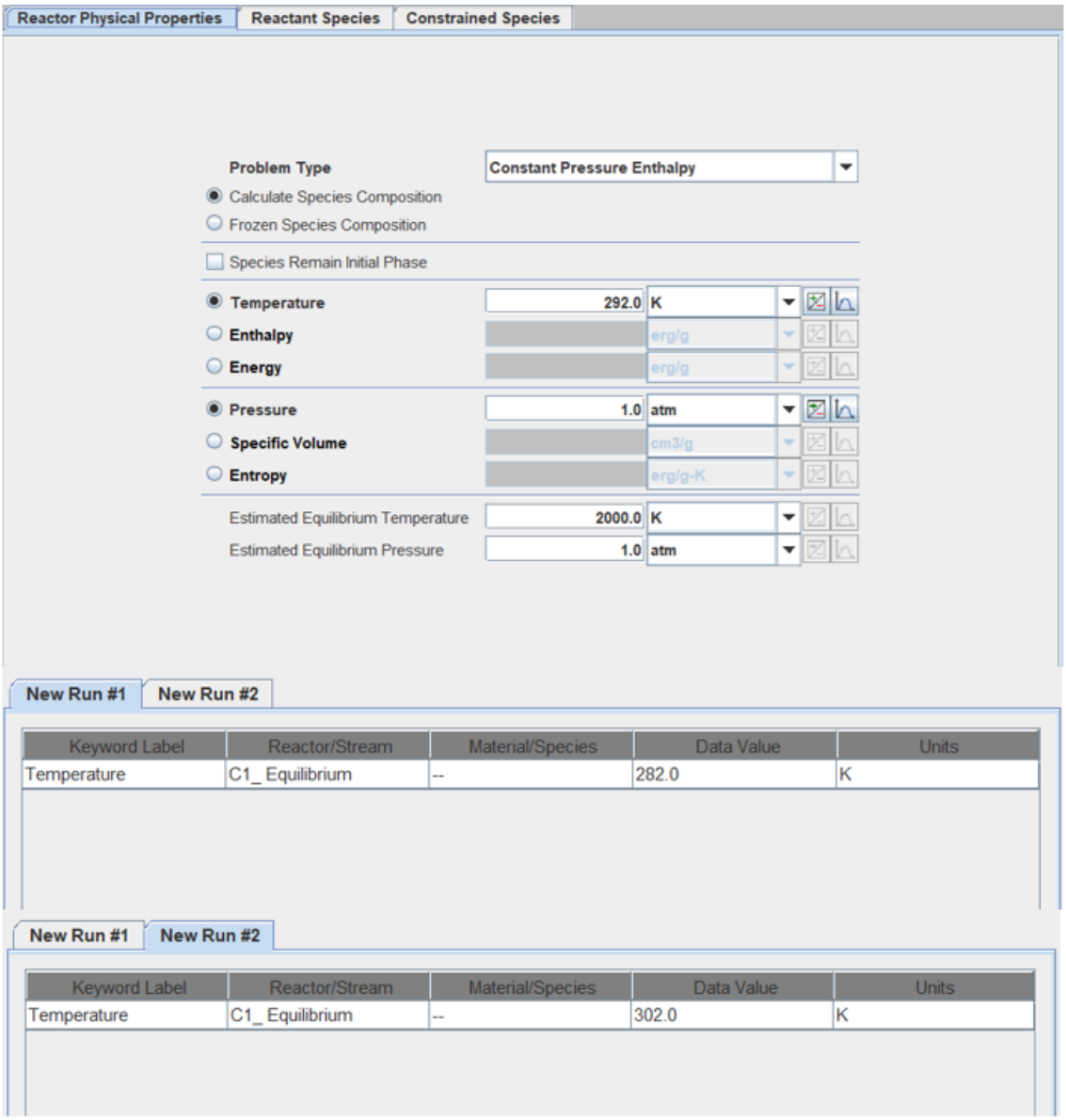

Figure 7.3 – Annex B | Adiabatic Flame Temperature | Simulation Parameters

7.2.2. Simulation Nº1 | 100% Natural Gas

Fuel Mixture | Oxidizer Mixture | Complete-Combustion Products | Added Species

Fuel Fraction of Total Fuel Species

Unit Selection: mole fraction (or mole)

Species | Data | Add

Species	Fuel Fraction of Total Fuel Species
C2H6	0.07
C3H8	0.017
CH4	0.9
CO2	0.007
H2	0
N2	0.006

Figure 7.4 – Annex B | Adiabatic Flame Temperature | Simulation Nº1 | Fuel mixture

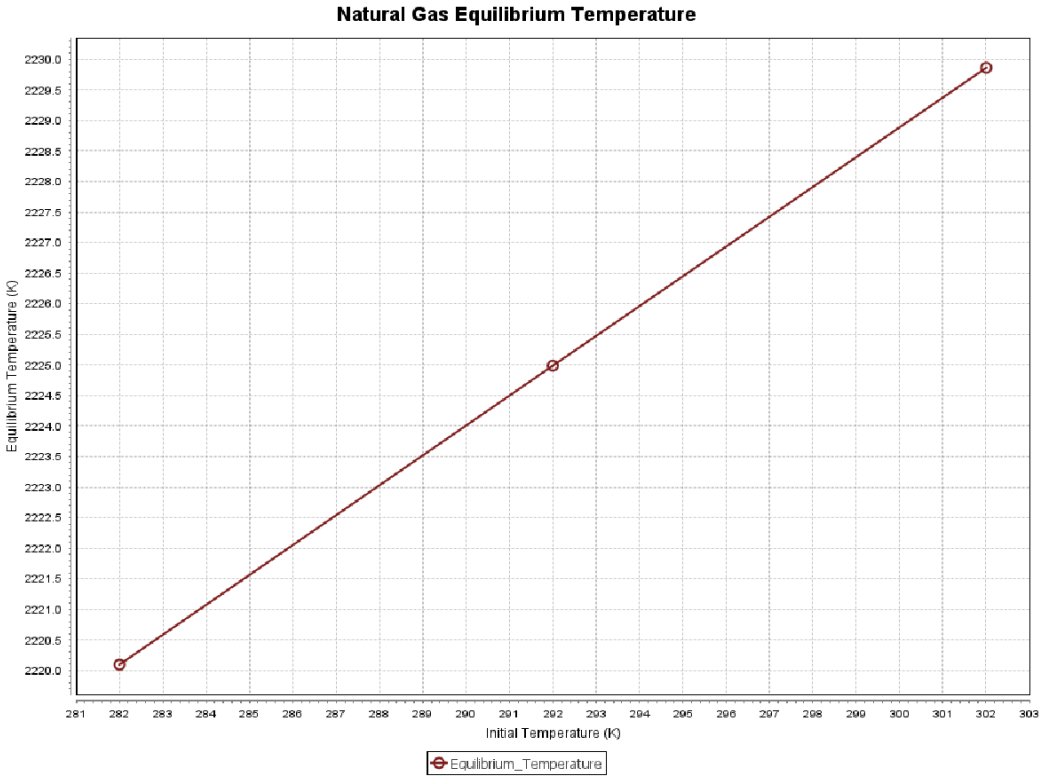

Figure 7.5 – Annex B | Adiabatic Flame Temperature | Simulation Nº1 | Results plotted

7.2.3. Simulation Nº2 | 75% Natural Gas – 25% Hydrogen

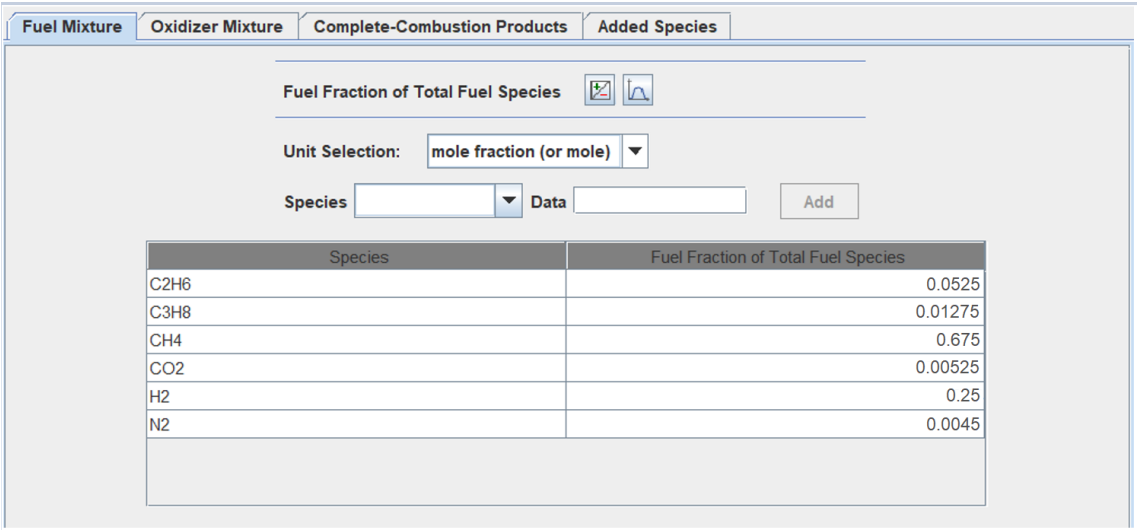

Species	Fuel Fraction of Total Fuel Species
C2H6	0.0525
C3H8	0.01275
CH4	0.675
CO2	0.00525
H2	0.25
N2	0.0045

Figure 7.6 – Annex B | Adiabatic Flame Temperature | Simulation Nº2 | Fuel mixture

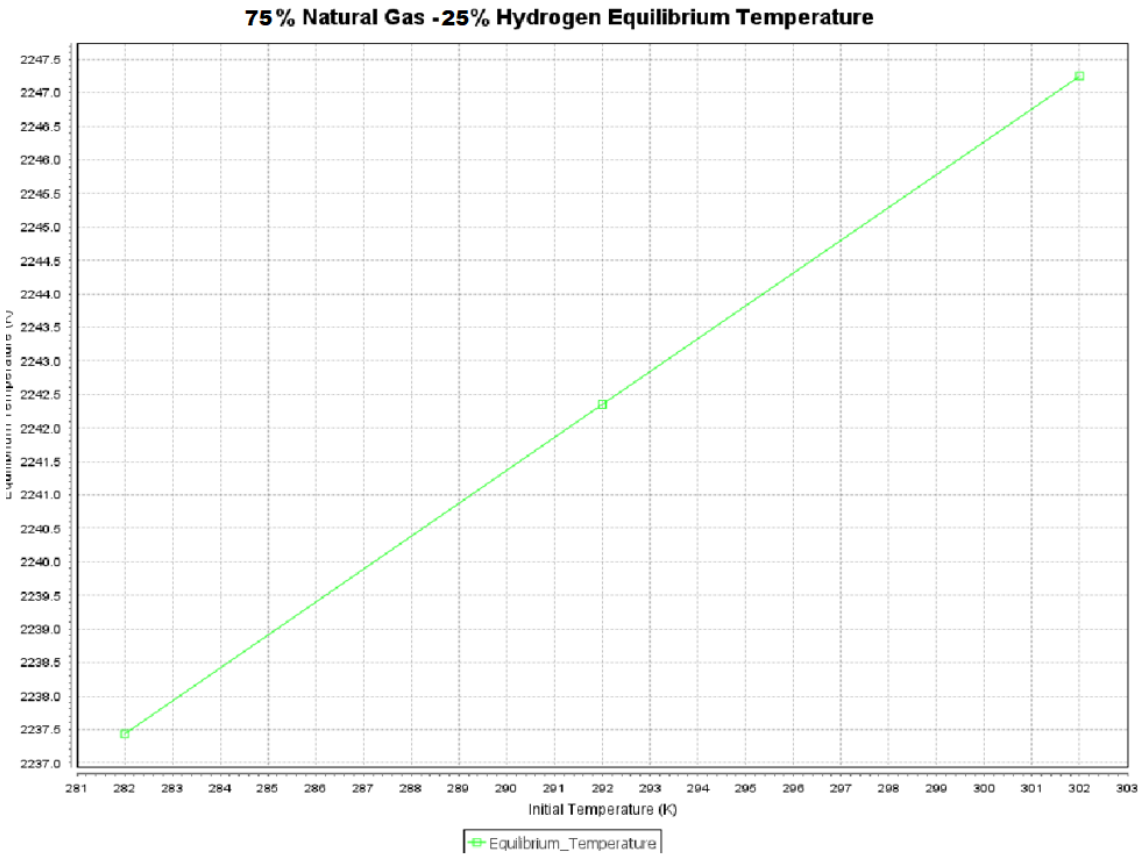

Figure 7.7 – Annex B | Adiabatic Flame Temperature | Simulation Nº2 | Results plotted

7.2.4. Simulation Nº3 | 50% Natural Gas – 50% Hydrogen

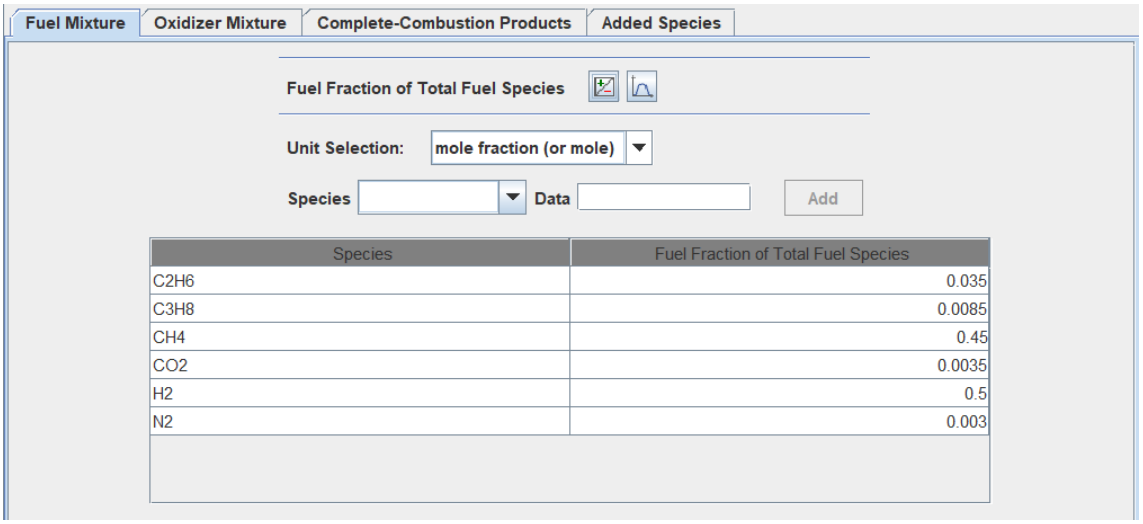

Species	Fuel Fraction of Total Fuel Species
C2H6	0.035
C3H8	0.0085
CH4	0.45
CO2	0.0035
H2	0.5
N2	0.003

Figure 7.8 – Annex B | Adiabatic Flame Temperature | Simulation Nº3 | Fuel mixture

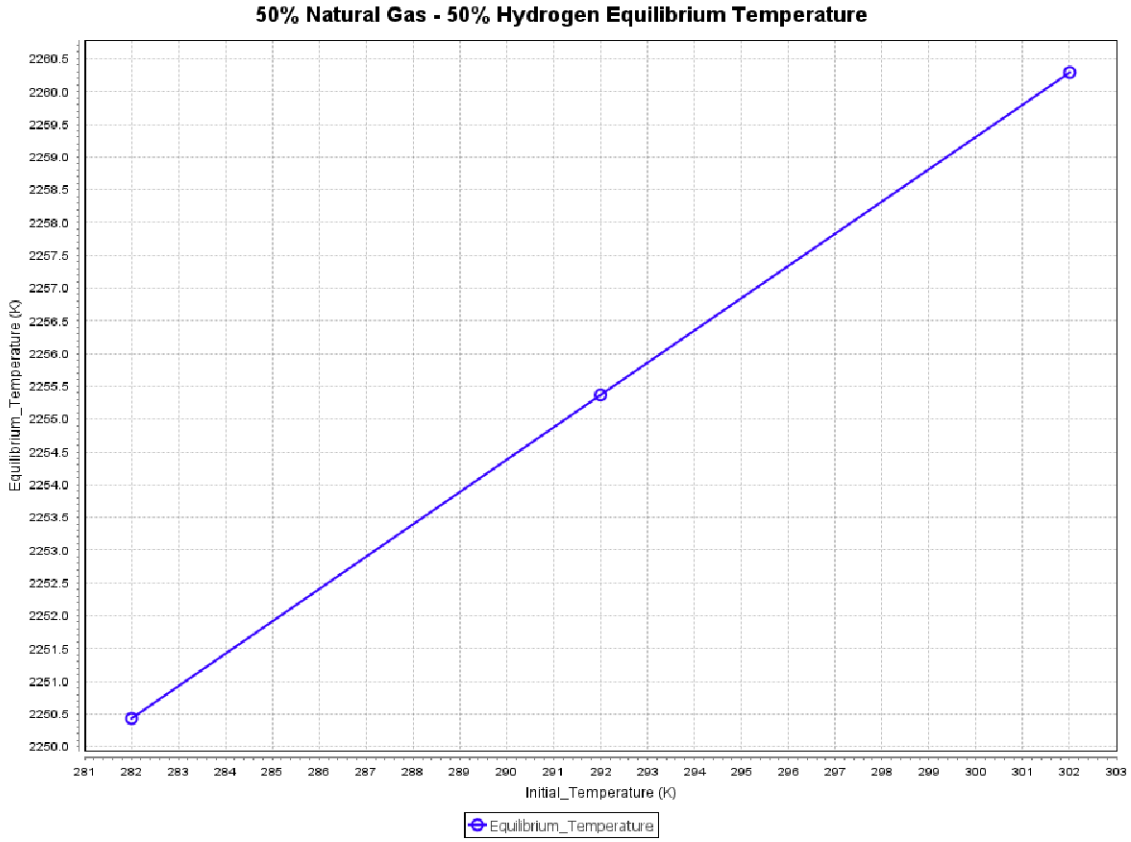

Figure 7.9 – Annex B | Adiabatic Flame Temperature | Simulation Nº3 | Results plotted

7.2.5. Simulation Nº4 | 25% Natural Gas – 75% Hydrogen

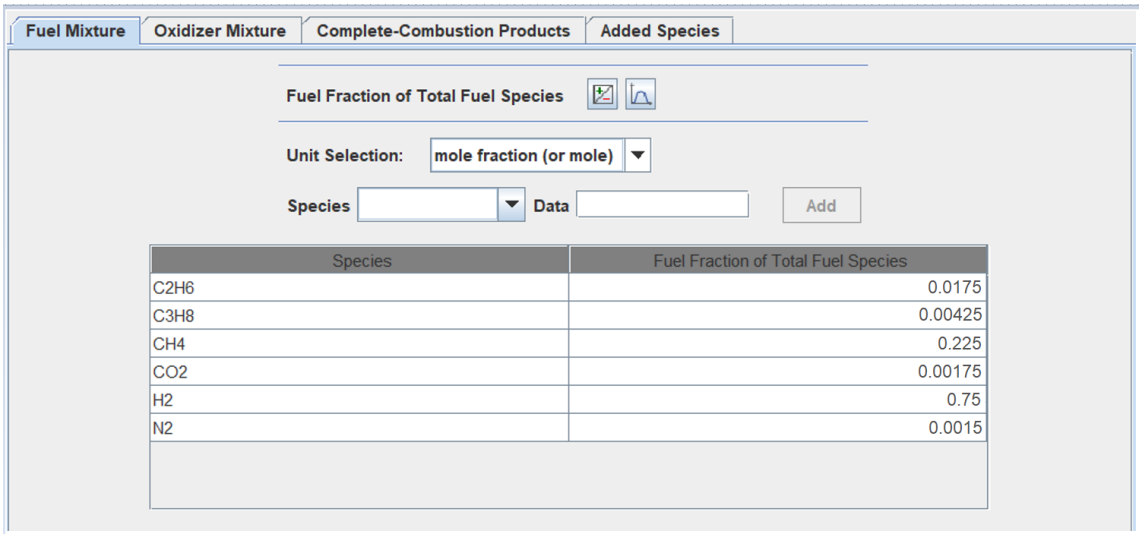

Species	Fuel Fraction of Total Fuel Species
C2H6	0.0175
C3H8	0.00425
CH4	0.225
CO2	0.00175
H2	0.75
N2	0.0015

Figure 7.10 – Annex B | Adiabatic Flame Temperature | Simulation Nº4 | Fuel mixture

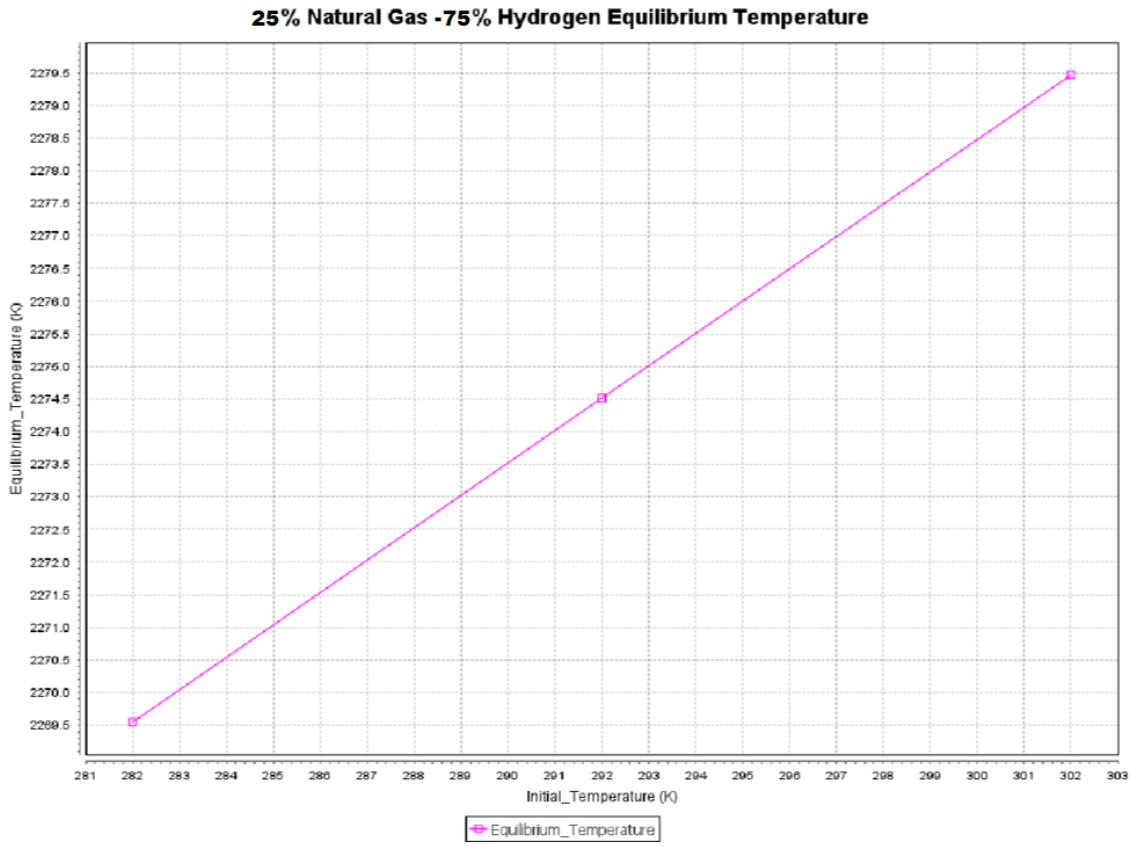

Figure 7.11 – Annex B | Adiabatic Flame Temperature | Simulation Nº4 | Results plotted

7.2.6. Simulation Nº5 | 100% Hydrogen

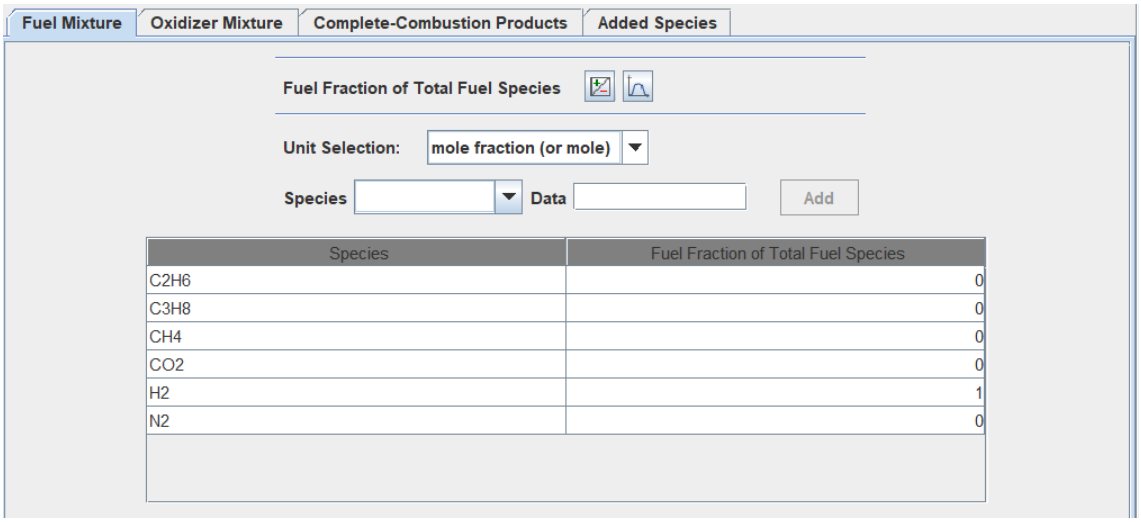

Figure 7.12 – Annex B | Adiabatic Flame Temperature | Simulation Nº5 | Fuel mixture

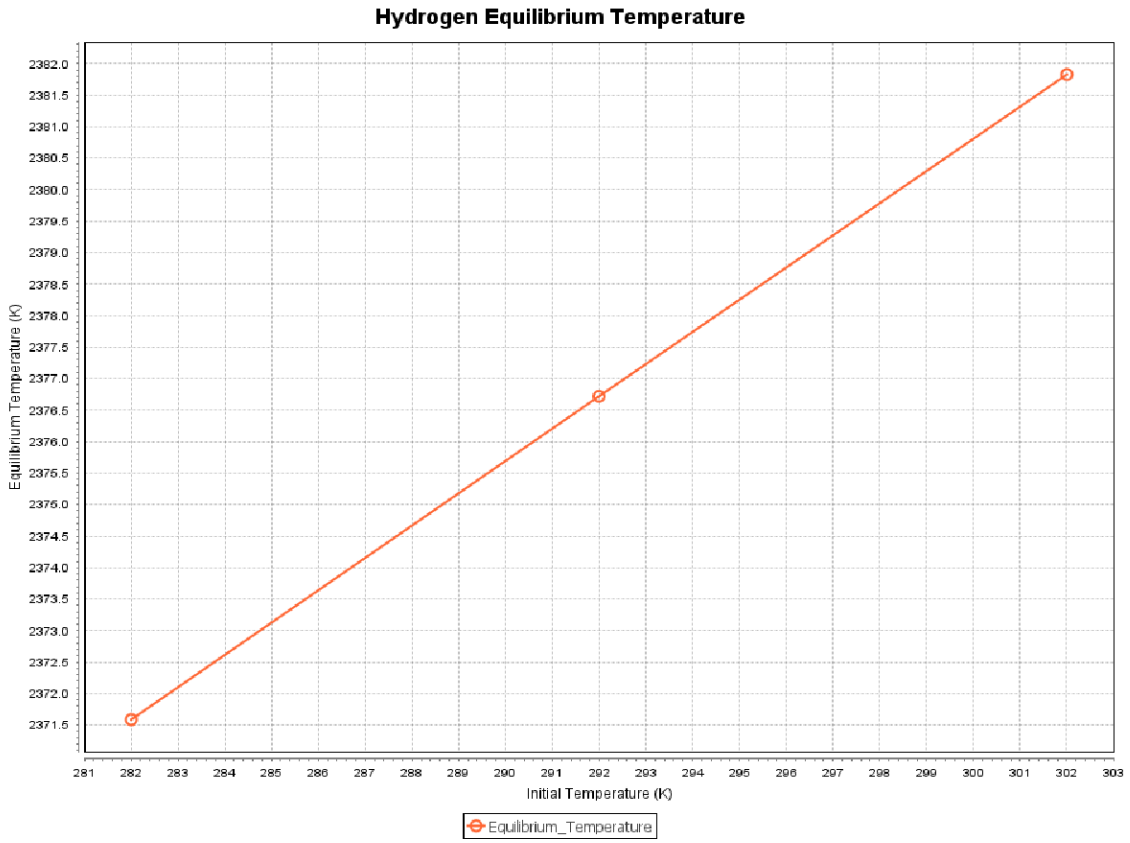

Figure 7.13 – Annex B | Adiabatic Flame Temperature | Simulation Nº5 | Results plotted

7.3. Annex C - Flame Speed Simulations

7.3.1. Flame Speed Simulation Parameters

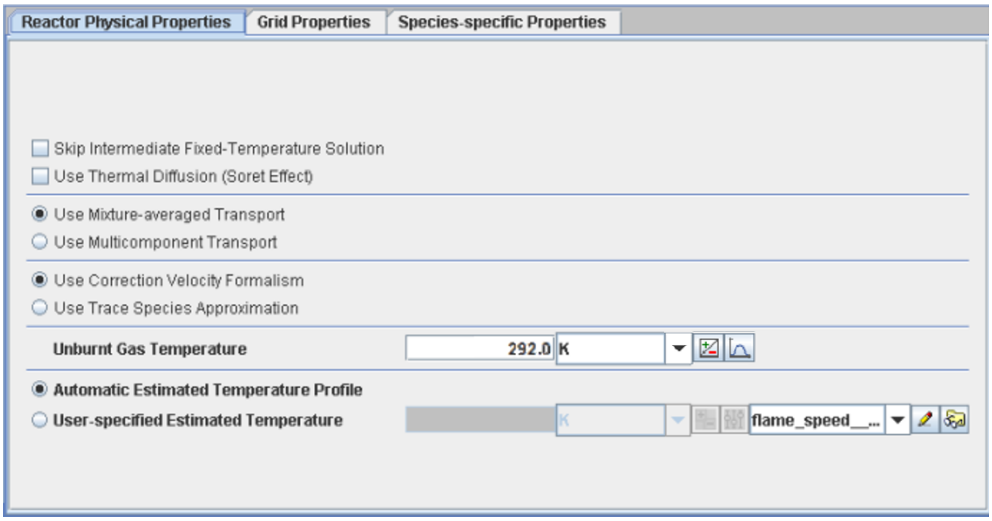

Figure 7.14 – Annex C | Flame Speed | Reactor Physical Properties

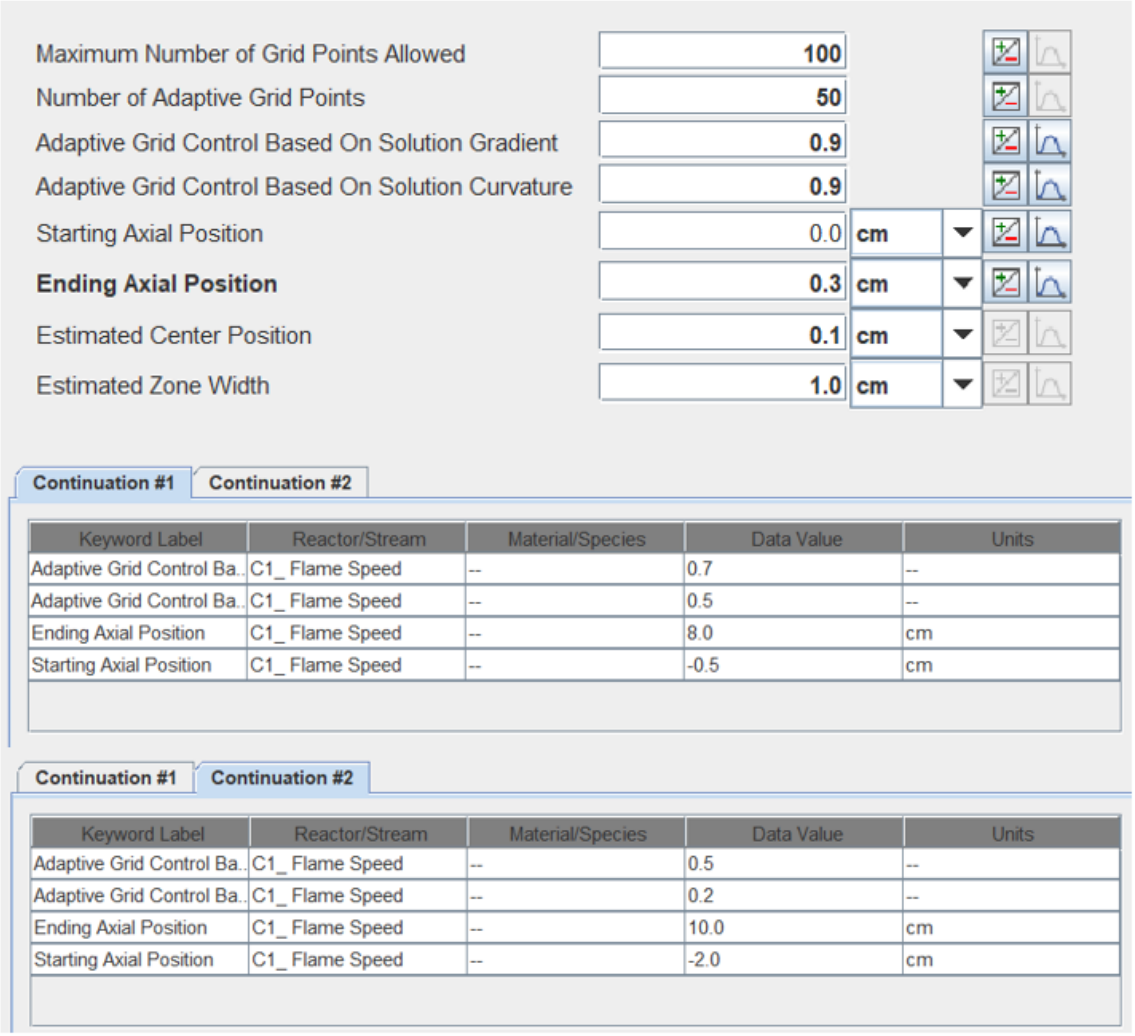

Figure 7.15 – Annex C | Flame Speed | Grid Properties

7.3.2. Simulation Nº1 | 100% Natural Gas

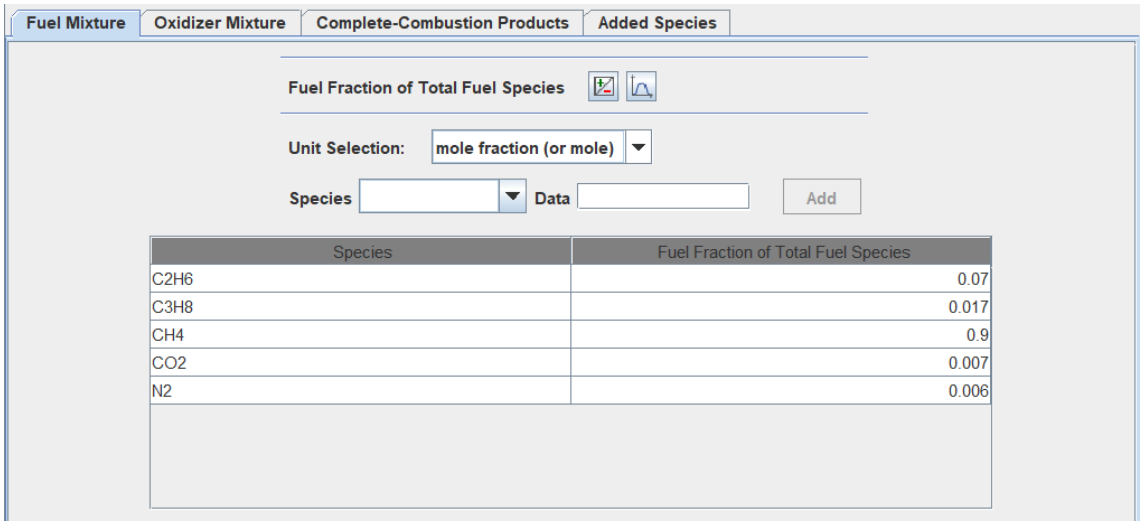

Species	Fuel Fraction of Total Fuel Species
C2H6	0.07
C3H8	0.017
CH4	0.9
CO2	0.007
N2	0.006

Figure 7.16 – Annex C | Flame Speed | Simulation Nº1 | Fuel mixture

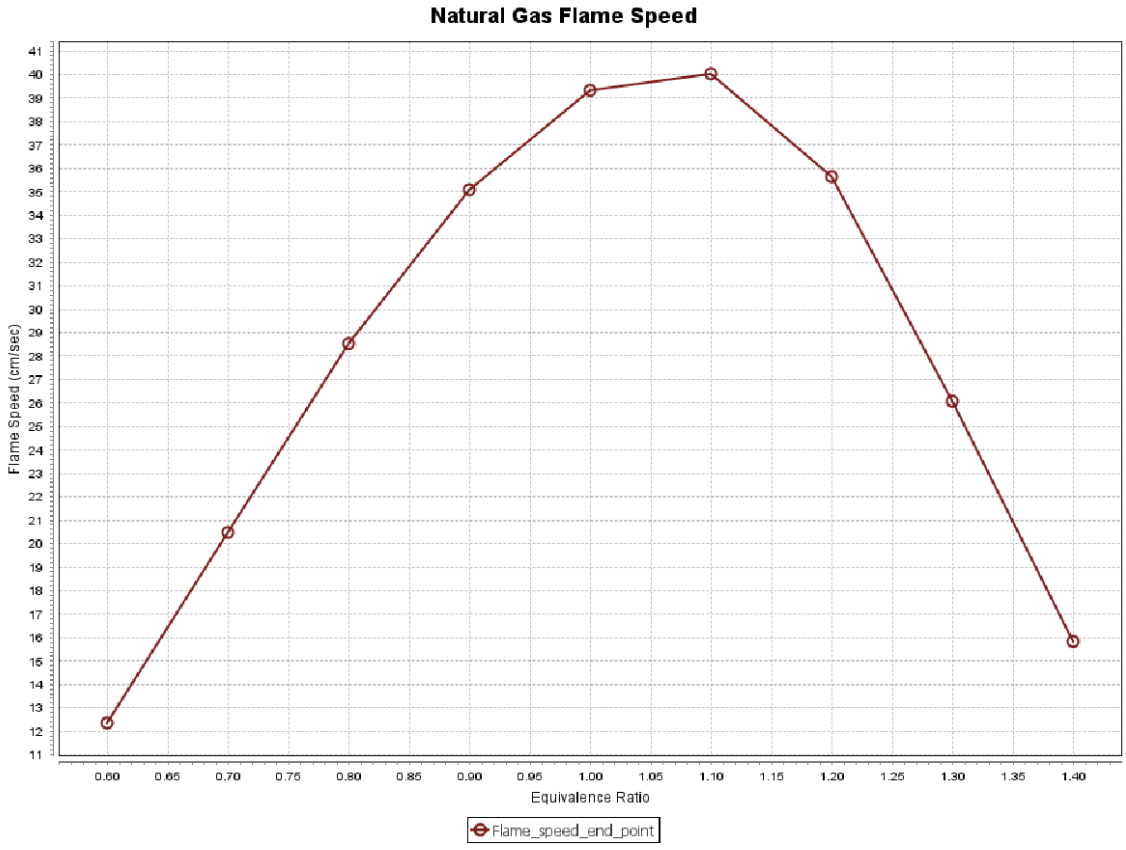

Figure 7.17 – Annex C | Flame Speed | Simulation Nº1 | Results plotted

7.3.3. Simulation Nº2 | 50% Natural Gas – 50% Hydrogen

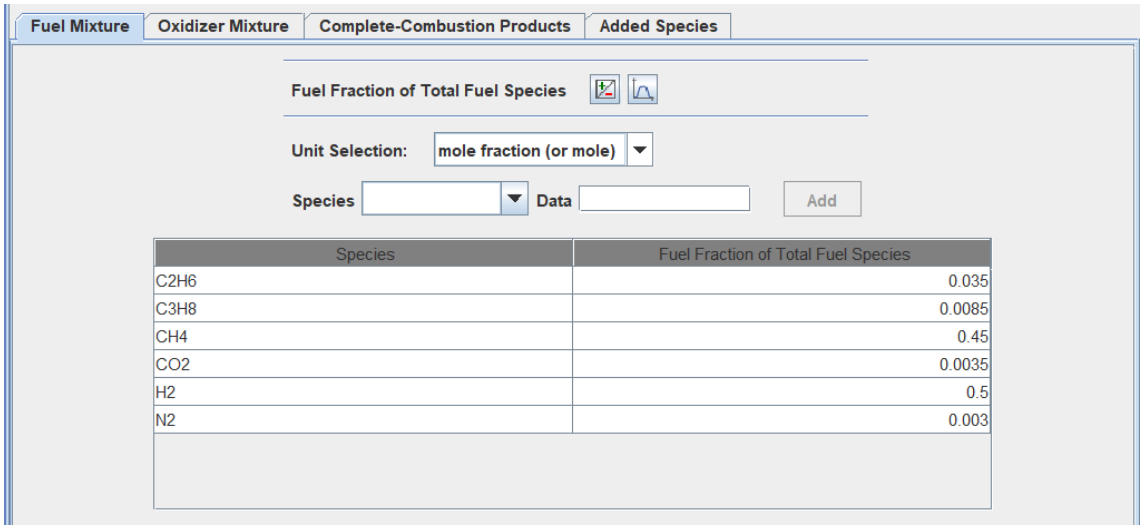

Species	Fuel Fraction of Total Fuel Species
C2H6	0.035
C3H8	0.0085
CH4	0.45
CO2	0.0035
H2	0.5
N2	0.003

Figure 7.18 – Annex C | Flame Speed | Simulation Nº2 | Fuel mixture

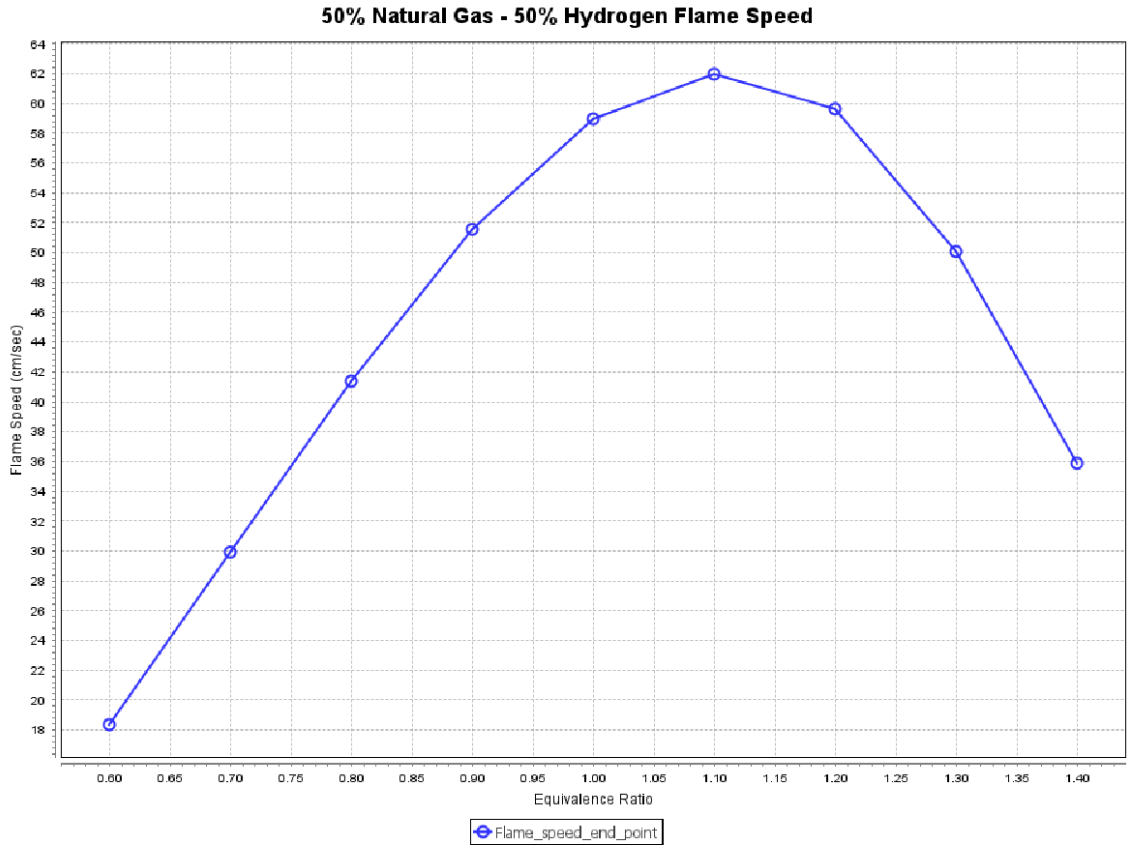

Figure 7.19 – Annex C | Flame Speed | Simulation Nº2 | Results plotted

7.3.4. Simulation Nº3 | 100% Hydrogen

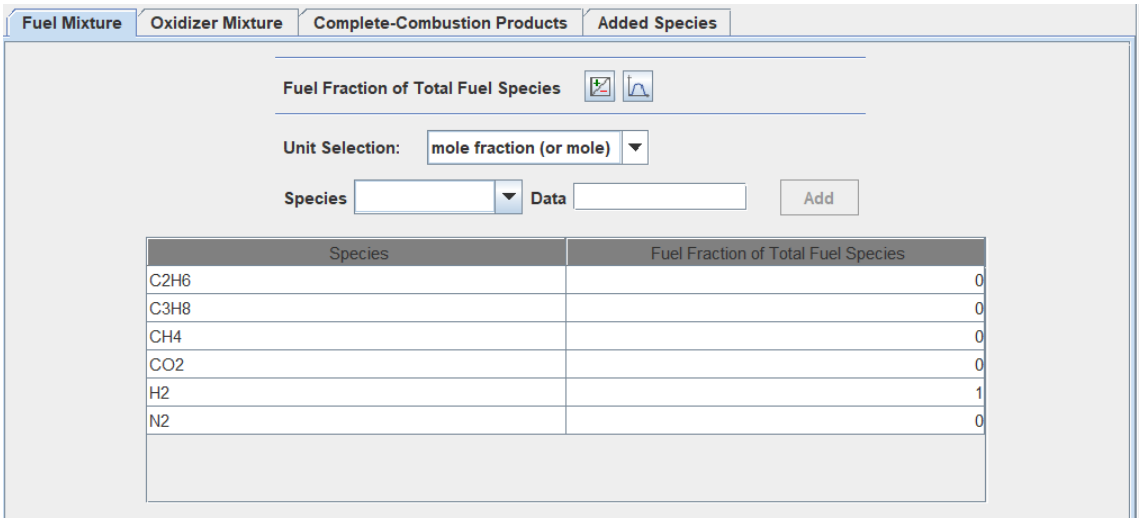

Species	Fuel Fraction of Total Fuel Species
C2H6	0
C3H8	0
CH4	0
CO2	0
H2	1
N2	0

Figure 7.20 – Annex C | Flame Speed | Simulation Nº3 | Fuel mixture

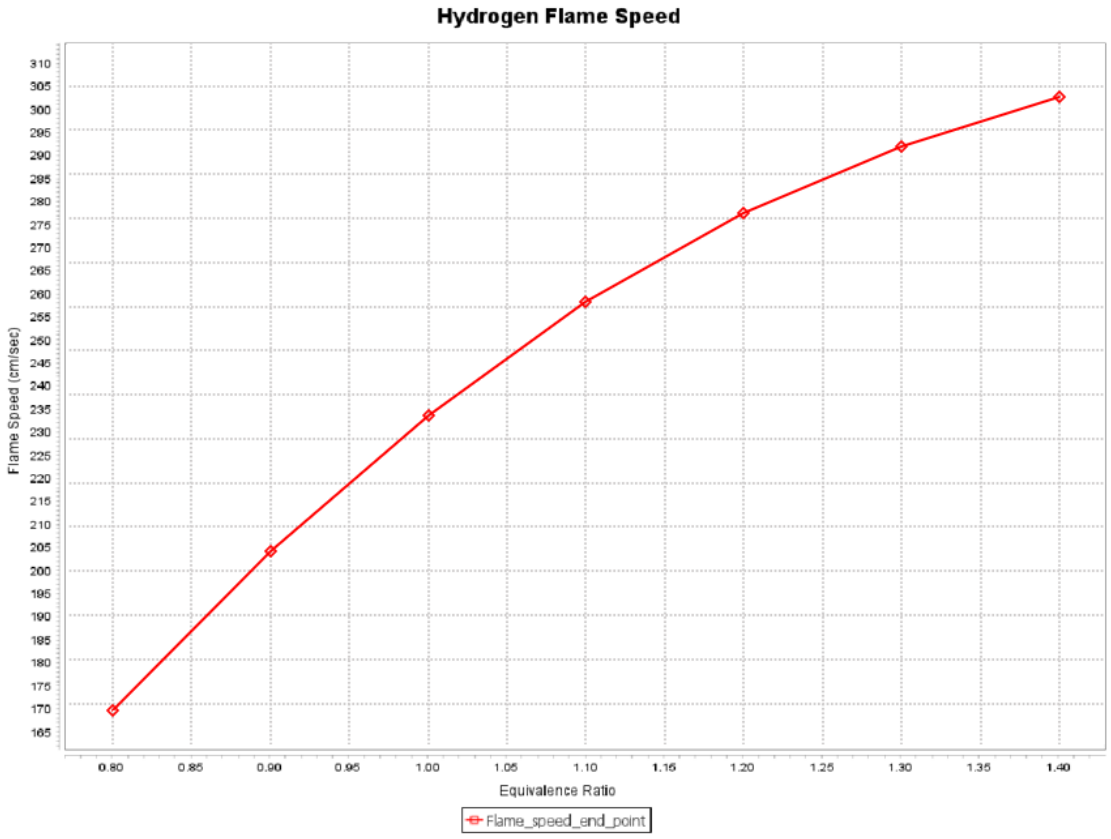

Figure 7.21 – Annex C | Flame Speed | Simulation Nº3 | Results plotted